
DIGITAL ACCESS TO SCHOLARSHIP AT HARVARD
DASH.HARVARD.EDU


HARVARD LIBRARY
Office for Scholarly Communication

Development of a Set of Standardized Toehold Switch Riboregulators and Fluorescent Reporter Proteins for Genetic Circuit Prototyping.

The Harvard community has made this article openly available. Please share how this access benefits you. Your story matters

Citation	Selvarajah, Vinoo. 2019. Development of a Set of Standardized Toehold Switch Riboregulators and Fluorescent Reporter Proteins for Genetic Circuit Prototyping.. Master's thesis, Harvard Extension School.
Citable link	https://nrs.harvard.edu/URN-3:HUL.INSTREPOS:37365394
Terms of Use	This article was downloaded from Harvard University's DASH repository, and is made available under the terms and conditions applicable to Other Posted Material, as set forth at http://nrs.harvard.edu/urn-3:HUL.InstRepos:dash.current.terms-of-use#LAA

Development of a Set of Standardized Toehold Switch Riboregulators and Fluorescent Reporter Proteins for Genetic Circuit Prototyping.

Vinoo Selvarajah

A Thesis in the Field of Biology

for the Degree of Master of Liberal Arts in Extension Studies

Harvard University

November 2019

Copyright 2019 Vinoo Selvarajah

Abstract

The goal of this research was the creation and characterization of a new library of Type IIS standardized biological parts that can be used to construct expression devices for reporter proteins with precise and reliable control. Toehold switches are one such element of control. As de-novo designed translational riboregulators, they can regulate ribosomal activity on an mRNA, thereby affecting post-transcriptional gene expression. Toehold switches act as a cognate pair of RNAs: the switch RNA interferes with ribosomal activity until a target RNA complementarily binds to the switch to allow for ribosomal binding and gene expression. For this research, eleven toehold switches were designed and constructed to be triggered by the target mRNA of a specific fluorescent reporter protein. The toehold switches were assembled with fluorescent reporter proteins, and these constructs were experimentally validated in a plate reader to determine toehold switch leakiness: demonstrating their efficacy in preventing translation of the downstream fluorescent protein. In total, 26 new basic parts, over 90 transcriptional units, eight multi-transcriptional units, and nine new assembly vectors were created that adhere to iGEM's Type IIS assembly standard, based on the previously defined MoClo and Loop standards. These parts and vectors allow for quick and reliable one-pot assembly of entire transcriptional units, or assemblies of multiple transcriptional units. This new library of Type IIS characterized part samples allows for quick prototyping of genetic circuit designs.

Acknowledgments

Thank you to all those that have helped me throughout this thesis project. I would like to sincerely thank my thesis directors, Dr. Traci Haddock-Angelli and Dr. Pamela Silver, my thesis advisor, Dr. James Morris, and the iGEM Foundation. Your support, patience, resources, and encouragement helped make this possible.

Finally, a heartfelt thank you to my family and friends who have helped and supported me along the way.

Table of Contents

List of Tables

List of Figures

Chapter I.

Introduction

Synthetic Biology Background

Synthetic biology uses engineering principles and perspectives to control biological systems and to build entirely de-novo biological machines. As a growing field, it has incredible potential for our ability to control matter on a molecular level: using organisms or biological-based systems to produce biofuels and useful materials, to build complex biological computers, or to work within the body to cure illnesses (Nielsen et al., 2013; Siuti et al., 2013; Chakravarti et al., 2016).

During the 1970s, several discoveries and improvements in the ability to manipulate DNA, including recombinant DNA, molecular cloning, and PCR, gave researchers the tools to start genetic engineering (Cameron et al., 2014). From the 1990s to this day, improvements in DNA sequencing, automation, and computation have allowed for the acceleration of the systems biology field, leading to the discovery and generation of large amounts of data on cellular systems, and interactions within and outside of cells (Cameron et al., 2014). The study of these complex systems led to their abstraction into smaller components and modules that could be isolated, defined, and characterized, as biological parts: nucleotide sequences that encode or perform discrete biological functions. This abstraction was crucial for the foundation of synthetic biology and its part-based approach to engineering with biology.

Synthetic biology's part-based approach led to the development of two simple genetic circuits that are considered milestones in the field: the genetic toggle switch and the repressilator, both of which were developed with a forward-engineering approach and a design-build-test philosophy (Gardner et al., 2000; Elowitz & Leibler, 2000). This included intentional design and modeling (design), DNA manipulation to physically construct their parts into genetic circuits (build), and subsequent characterization of their circuits and debugging (test), which led to iterative design improvements (Cameron et al., 2014). As forward-engineered genetic circuits designed to work in *E. coli*, the toggle switch and the repressilator relied on well-characterized promoters and repressors as transcriptional control elements for gene regulation.

Biological Parts

The toggle switch and repressilator were designed and constructed with a similar set of biological parts that are ubiquitous in synthetic biology (Cameron et al., 2014). Fluorescent reporter proteins, like green fluorescent protein (GFP), are widely used in the field and have proven to be an invaluable type of part for synthetic biologists, especially when designing new genetic circuits. GFP and other fluorescent reporter proteins are often used as a visual indicator to test and measure how regulation of a genetic circuit is working, and they can later be replaced by another gene of interest.

Both the toggle switch and repressilator also used well-characterized and orthogonal repressor-promoter sets, such as the TetR repressor and its cognate promoter pTetR. Orthogonality is a property by which a component or system is independent of effects to and from other components. In this case, the repressilator relied on three highly orthogonal repressor-promoter interactions that would not unintentionally affect each

other, allowing for stable oscillation of GFP within a cell. These parts could also be replaced with a different set of orthogonal repressor-promoters, while still maintaining the desired function of the device (Elowitz & Leibler, 2000). The development of the toggle switch and repressilator demonstrated how a synthetic biologist could build completely different genetic circuits with a relatively small set of characterized, orthogonal, and reliable biological parts. However, as we move into the future, or "second wave," of synthetic biology, we need more of these regulatory elements in order to increase the control and complexity of genetic circuits and to build systems-level designs (Purnick & Weiss, 2009).

Creating new well-characterized, orthogonal, and reliable parts is a continuous activity within synthetic biology. Its importance can be seen in the development of a library of TetR orthologs, designed specifically to allow for greater complexity in genetic circuit design with low cross-talk between circuits (Stanton et al., 2013). By mining prokaryotic genomes and building a library of TetR repressors, the authors were able to generate synthetic promoters and repressors, which were then screened for strength of repression and orthogonality. Sixteen of these were selected, converted, further characterized, and used to build complex circuits (Stanton et al., 2013). Their work represented a large set of orthogonal regulatory elements where gene expression can be tightly regulated through transcriptional control, allowing users to build complex circuits.

Translational Control Elements

Synthetic biologists have also generated new regulatory elements for translational control, as these parts offer additional methods for precision and complexity in gene expression and genetic circuit design. After transcription of a DNA sequence into mRNA,

expression of a gene can then be controlled by affecting said mRNA strand before it has been translated into protein. Classically, this has been achieved by mutating the ribosome binding site (RBS) on the mRNA strand, to either increase or decrease the ribosomes affinity to bind the strand, thereby affecting the translation of the protein (Purnick & Weiss., 2009). However, additional control mechanisms have been developed by studying RNA-based regulatory elements. These regulatory elements are common in prokaryotes, many of which use antisense RNAs that can affect translation by complementarily binding mRNA and altering secondary structure formation (Brantl & Wagner., 2002; Mizuno et al., 1984). RNA-based regulatory elements have inspired new biological parts, such as translational riboregulators. These parts are designed to regulate ribosomal activity on a mRNA strand, thereby affecting gene expression, independently or in conjunction with other regulatory elements like promoters (Isaacs et al., 2004).

The translational riboregulator developed by Isaacs et al. consists of a cognate pair of RNA (Figure 5A). The cis-repressive sequence (crRNA) forms a secondary structure with the ribosomal binding site (RBS). When transcribed as mRNA, the upstream 5′– crRNA contains a short sequence that is complementary to the RBS sequence, forming a stem-loop secondary structure which sequesters the RBS (Figure 5A, shown in blue) (Isaacs et al., 2004). This prevents the ribosome from binding and represses translation of the downstream coding region. However, when Isaacs et al., introduce a trans-activating small noncoding RNA (taRNA) it complementarily binds to the crRNA. This will create a conformational change in the stem-loop structure to allow for ribosomal binding and translation of the downstream protein coding sequence, GFP in this example (Figure 5A) (Isaacs et al., 2004). While functional as a regulator, Isaac's

riboregulator design does not have a high degree of dynamic range or orthogonality, and also has sequence limitations between the crRNA and taRNA (Figure 5A) (Green et al., 2014).

Toehold Switches

Toehold switches, developed by Green et al., were designed to overcome the limitations of traditional riboregulators. Toehold switches are based on the same Watson-Crick base pairing process of other riboregulators, but their mechanism for controlling gene expression is completely artificial (Green et al., 2014). The complementation between the switch RNA and trigger RNA does not use the RBS, which now resides in the loop of the stem-loop (Figure 5B, shown in blue). This was an intentional design change, as the authors found that it would result in a linear-linear interaction between the cognate pair, as opposed to the loop-linear interaction in a conventional riboregulator. Comparatively, the linear-linear interaction is kinetically and thermodynamically favorable, allowing for a higher dynamic range of regulation, similar to that of well-characterized promoters (Green et al., 2014). Additionally, there are fewer sequence restrictions for the pair, allowing for greater orthogonality as the interaction between the switch and trigger can be based on arbitrary sequences (Figure 5B) (Green et al., 2014).

With these design improvements, Green et al. were able to engineer and test a set of 26 highly orthogonal toehold switches. They demonstrated the high dynamic range of each toehold switch by measuring GFP expression; when a switch was activated by its cognate trigger, it would undergo conformational change to allow for translation of the downstream GFP mRNA. To measure orthogonality, they used GFP expression once again. When a switch was in the presence of a non-cognate trigger, low or no GFP

expression meant it was orthogonal; the switch was not unintentionally activated and allowing for translation of the downstream GFP mRNA. Finally, Green et al. used a subset of toehold switches to independently regulate a system of 12 genes and to build biological logic gates, demonstrating how useful their de-novo riboregulators were to synthetic biologists.

To further showcase the abilities of toehold switches, Green et al. also designed a set that used another fluorescent protein, mCherry, to demonstrate a complete mRNA strand functioning as the trigger. This set of toehold switches would allow for translation of GFP, only in response to an mCherry mRNA trigger (Green et al., 2014). By using both GFP and mCherry, the authors had two separate visual indicators and measurable quantities to characterize the robustness of their riboregulator.

Characterization and Standard Measurements

The way biological parts are tested and characterized matters greatly. A major issue faced by synthetic biologists is a lack of standardized measurement protocols so that experiments are consistent and repeatable, and their data is truly comparable (Beal et al., 2018). In synthetic biology, fluorescence measurements have often been reported in relative units as either arbitrary units (a.u.) or normalized against a control, producing data specific to the experiment without comparable units (Beal et al., 2018). Notably, the repressilator and genetic toggle measured GFP expression in arbitrary units (a.u.) and normalized relative units, respectively (Elowitz & Leibler, 2000; Gardner et al., 2000). Even the more recent work on TetR orthologs measured YFP expression in normalized relative units (Stanton et al., 2013).

The Interlab Measurement study conducted by iGEM teams has helped address this issue through the creation and evolution of a standardized protocol for measuring green fluorescent protein in a plate reader with the use of calibrants (Beal et al., 2016; Beal et al., 2018). Starting in 2014, the iGEM Interlab Study sought to ask how research labs from around the world were measuring GFP fluorescence, and finding that few participants were able to measure fluorescence in absolute units (Beal et al., 2016). Of those participants that were able to use absolute units, Beal et al. still found large differences between the data values, which they attributed to differing or incorrect calibration techniques between participants (Beal et al., 2016). By introducing calibrants and process controls, as well as a more specific protocol, participants in more recent InterLab studies were able to generate data with comparable units and better precision (Beal et al., 2018). As an engineering discipline, measurements that are consistent, repeatable, and comparable are essential to the characterization of parts and the creation of predictable genetic circuits.

Type IIS Assembly

Assembly standards are a type of framework that allow synthetic biologists to build their systems quickly and reliably. The BioBrick assembly standard was the earliest established assembly standard in synthetic biology. Developed by Tom Knight in 2003, it supported the concept of standard biological parts by introducing specific requirements for their DNA sequences. The BioBrick standard allows for restriction enzyme based assembly with a focus on idempotency: the key structural elements that allow for assembly are maintained after the assembly reaction (Knight, 2003). Two BioBrick parts could be assembled together, and the new resulting composite part would adhere to the

standard and maintain the required restriction sites need for subsequent assemblies (Knight, 2003).

Early assembly standards, like the BioBrick standard, were absolutely vital to the growth of the field. While it is still used today, it has clear limitations: as an example, only two BioBrick parts can be assembled in a single reaction. Newer assembly standards have tackled such issues (Ellis et al., 2011). Modular Cloning (MoClo), developed in 2011, improved upon this concept: allowing for efficient one-pot assembly of multiple DNA fragments at a time (Weber et al., 2011). Based on the GoldenGate method, this assembly standard uses Type IIS restriction enzymes, which can indiscriminately cleave DNA a defined distance from their their asymmetrical recognition sequence (Engler et al., 2008; Weber et al., 2011). This allows MoClo users to dictate intentional overhangs flanking each fragment, or part, so that they can ligate multiple parts together in a specified direction and location (Weber et al., 2011).

Several Type IIS assembly standards have been created since MoClo, and many of these build upon it to allow for cross compatibility of parts and samples (Iverson et al., 2016; Patron et al., 2015). Loop assembly is one such assembly standard; it supports MoClo part samples for basic parts (Level 0s), and dictates the assembly of transcriptional units (Level 1s) and multi-transcriptional units (Level 2s) (Pollack et al., 2018). By "looping" between two assembly vectors, the Loop assembly method allows users to build large genetic circuits, by alternating between two Type IIS restriction enzymes (Figure 6) (Pollack et al., 2018). Lastly, the Loop assembly method and its assembly vectors are provided under an OpenMTA license, placing them in the public domain and allowing them to be freely distributed (Pollack et al., 2018).

While the iGEM Registry (http://parts.igem.org) continues to support the BioBrick standard, it has also since adopted a Type IIS Standard based on Loop and MoClo (Type IIS, 2019). The creation of a library of well-characterized Type IIS parts and vectors would increase the samples that are currently available to the community.

Research Goals

The objective of this thesis is the development of a new library of Type IIS standardized biological parts that can be used to construct expression devices with translational control elements that offer precision and predictability. Based on previous work by Green et al., it is hypothesized that a set of standardized toehold switches can act as these translation control elements in response to their cognate mRNA sequence with high specificity and orthogonality. To test this hypothesis, new basic parts samples, specifically toehold switches and fluorescent reporter proteins, along with Type IIS assembly vectors will be designed and generated. Using Type IIS assembly, these parts will then be assembled into test constructs.

Toehold constructs, consisting of a toehold switch paired with a fluorescent reporter protein, will be experimentally validated in a plate reader to test leakiness: demonstrating the toehold switch's efficacy in preventing translation of the downstream fluorescent protein when in the "off" state. These toehold switch constructs will then be assembled with target mRNA constructs that produce either their cognate trigger mRNA or a non-cognate sequence. Finally, these multi-transcriptional units will be experimentally validated in a plate reader to test specificity and orthogonality, whether they fluoresce in response to their cognate trigger mRNA or non-cognate mRNAs. All characterization work will use a standardized measurement protocol based on the iGEM

Interlab study, to increase experimental precision and repeatability, and generate characterization data with comparable units.

Chapter II.

Materials and Methods

Overview

This research evaluated the use of toehold switches as translational control elements in fluorescent protein expression constructs. This included the creation and characterization of a library of Type IIS parts for assembling these constructs, and as a resource for potential future work. New basic parts (Level 0s), transcriptional units (Level 1s), multi-transcriptional units (Level 2s), and assembly vectors were designed and constructed in order to test toehold switch design. All parts and assembly vectors conformed to iGEM's Type IIS assembly method based on MoClo and Loop (Type IIS, 2019; Weber et al., 2011; Pollack et al., 2018). All sequences of Type IIS parts and assembly vectors were designed and verified in Benchling (http://benchling.com). Finally, once assembled, toehold switch constructs were experimentally validated in a plate reader following a calibrated protocol using fluorescent standards (Beal et al., 2018). Statistical analysis was used to determine toehold switch leakiness, meaning their ability to prevent translation of a downstream fluorescent protein in the absence of their target mRNA.

Assembly Vector Design

Three types of assembly vectors were designed for Type IIS assembly: a Universal Acceptor Plasmid (pSB1C00) to clone and maintain new Level 0 (basic) part samples, four Level 1 plasmids (pSB1K01-4) to assemble Level 0 parts into transcriptional units, and four Level 2 plasmids (pSB3C01-4) to assemble Level 1 transcriptional units into multi-transcriptional units. All plasmids were based on BioBrick plasmids obtained from the iGEM Registry (http://parts.igem.org). BBa_J04450, a red fluorescent protein (RFP) generator device, was used as the selection marker in all assembly vectors ("BBa_J04450," 2005). When Type IIS parts are assembled into these plasmids, BBa_J04450 was used to select against correct assemblies.

The design of pSB1C00 was based on the PhytoBricks Universal Acceptor Plasmid that allowed users to digest and ligate compatible inserts with the desired Level 0 Type IIS fusion sites (Figure 7) (Patron et al., 2015). The major design difference is that pSB1C00 uses SapI, instead of BsmBI, to clone part samples into the cloning site. This was done in order to keep the illegal restriction sites used in the iGEM's Type IIS assembly method at two (SapI, BsaI) instead of three (SapI, BsaI, BsmBI). pSB1C00 was built upon pSB1C3, a high-copy BioBrick chloramphenicol-resistant backbone ("pSB1C3," 2008). High-copy was desired as only basic parts are maintained in this vector.

Level 1 and Level 2 Type IIS assembly vectors were designed based on the cloning sites of the pOdd and pEven Loop vectors, respectively (Pollack et al., 2018). All four pOdd plasmids (pSB1K01-4) were built upon pSB1K3, a high-copy BioBrick kanamycin-resistant backbone ("pSB1K3," 2008). High-copy was desired as only a single

transcriptional unit is maintained in this vector. All four pEven-based plasmids (pSB3C01-4) were built upon pSB3C5, a medium-copy BioBrick chloramphenicol-resistant backbone ("pSB3C5," 2007). A medium-copy plasmid was desired as multi-transcriptional unit constructs would likely tax cells too much in a high-copy one.

Three sets of forward and reverse primers were designed to amplify BBa_J04450 with overhangs that included the required cloning site for the three Type IIS assembly vectors. EcoRI and PstI recognition sites were included on these primer overhangs. BBa_J04450 was used as template in a PCR reaction with each set of primers (see details below). PCR product was purified and quantified. The PCR product was then cloned into the BioBrick plasmids with an EcoRI and PstI digest, subsequent ligation, and transformation (see details below). Plasmids were then sequence verified at the cloning site using the VF and VR primers, located in all pSB vectors.

Toehold Switch Design

Eleven toehold switches were designed based on the parameters set in Green et al. for targeting mCherry mRNA (Figure 5B). This included use of the same RBS loop, hairpin structure spacing, and amino acid linker (Figure 8). Fluorescent reporter protein sequences were aligned in Benchling in order to determine uniquely heterologous sequences between them. Target sequences for toehold switches were selected based on a minimum of 20 base pairs sequences with less than 50% similarity when compared to related fluorescent proteins. After selection, target sequences were extended to 30 base pairs, and the complementary sequence was used in the toehold design (Table 9). Finally, designs were validated through NUPACK online (http://www.nupack.org) software to determine desired hairpin structure within the toehold switch. Additionally,

one control toehold switch (BNonTS) was designed, which included the RBS loop sequence and linker sequence but no target sequence or hairpin structure, with the expectation that it would not inhibit translation of downstream mRNA (Table 9). Toehold switch samples were constructed through oligo annealing and extension, followed by insertion into pSB1C00, transformation, and sequencing for verification (see details below).

Spacer Design

Level 2 (pEven) Loop constructs require four Level 1 parts for a successful assembly (Figure 6). When fewer than four Level 1 parts are needed for a multi-transcriptional device, spacers can be used to fill in as non-transcribed Level 1 parts to complete an assembly and to add space between constructs. Four spacer sequences were selected for this purpose (Table 10). While not used in the same context for this research, these 36 base pair spacers were shown to insulate promoter sequences, specifically BBa_J23100, from potential effects to expression caused by upstream DNA sequence (Carr et al., 2017). Spacers were made with oligo annealing, followed by insertion into pSB1K0X assembly vectors, transformation, and sequencing for verification (details below).

Existing Type IIS Part Samples

The iGEM Registry contained several sequence verified Type IIS Level 0 part samples, specifically promoters and ribosome binding sites, that required no further modification (Table 11). These samples were streaked onto selective LB agar plates for

overnight incubation, in order to prepare cell cultures for plasmid extraction (see details below).

New Type IIS Part Samples

Many of the basic parts used in this research were sourced from the iGEM Registry. Some of these parts, specifically reporter proteins and terminators, had sequence verified samples in BioBrick format in the Registry (Knight, 2003). For this research, these parts needed new samples standardized to Type IIS Level 0 format. PCR was used to take existing part samples and make the necessary modifications to create new Type IIS samples.

BioBrick samples were streaked onto LB agar plates for overnight incubation, and then cell cultured for plasmid extraction (see details below). The plasmid DNA was then used as template in PCR reactions. Forward and reverse primers were designed for each part, to bind with the template at the desired sequence (18-24bp on each end) and to have overhangs that contained the required fusion sites and enzyme sites (SapI) for cloning into pSB1C00. After PCR (see below for details), PCR product was cloned into pSB1C00, transformed, and sequence verified.

PCR Protocol

The following protocol was used for the creation and amplification of Type IIS Level 0 parts and for assembly vectors. All primers were analyzed through IDT's Oligo Analyzer (https://www.idtdna.com/calc/analyzer) to calculate melting temperature and check for hairpin, homodimer, and heterodimer structures that may adversely affect PCR reactions. Primers were purchased from Thermo Fisher, resuspended with sterile

deionized water (diH_2O) at a concentration of 100 µM, and diluted to working stocks of 20 µM. PCR master mix was purchased from Thermo Fisher (catalog no. 12532016). The temperature of the annealing step (Step 3, Table 2) was adjusted as needed according to the melting temperature (3-5°C below melting temperature) of the primers.

PCR product was used directly in a cloning reaction (details below), or stored at -20°C for later use. In some cases, PCR product was purified before use with a Qiagen PCR Purification kit (catalog no. 28104) following the vendor's protocol, quantified on a Nanodrop, and diluted to 15 fmol with diH_2O.

Table 1. Single PCR Reaction (50 µL).

Volume	**Reagent**
2.0 µL	Forward Primer (20 µM)
2.0 µL	Reverse Primer (20 µM)
1.0 µL	Template DNA (10-100 ng)
45 µL	PCR SuperMix

Setup for a single PCR reaction.

Table 2. PCR Protocol.

Step	**Temperature**	**Time**	**Cycles**
1	95°C	3 min	
2	95°C	30 sec	Cycle steps 2 – 4 (30 – 24 times)
3	55°C - 68°C	30 sec	
4	68°C	1 min	
5	68°C	10 min	
6	4°C	Hold	

Thermocycler settings for all PCR reactions.

Oligo Annealing and Extension

New Type IIS Parts that were under 140 base pairs and did not have a pre-existing DNA sample in the iGEM Registry were made through oligo annealing and extension. Forward and reverse oligos for each part were designed to have at least 20 base pairs of overlap so that they could bind to each other. The oligo overhangs included the remainder of the part's sequence, the desired Type IIS fusion sites, and the enzyme sites for cloning into the assembly vector (SapI for pSB1C00, BsaI for pSB1K0X). Oligos were analyzed through IDT's Oligo Analyzer (https://www.idtdna.com/calc/analyzer), and purchased from Thermo Fisher (https://www.thermofisher.com). Once received, oligos were annealed using the following protocol (Annealing and primer extension, 2006), and product was used directly in an assembly reaction (details below).

Type IIS Assembly Reactions

The protocol for Type IIS assembly reactions followed a hybrid of the protocol established by Boston University's CIDAR MoClo and Loop Assembly (Iverson et al., 2016; Pollack et al., 2018). For all Type IIS assemblies, plasmid DNA for parts was diluted to 15 fmol and destination plasmid was diluted to 7.5 fmol. In some cases, however, PCR or oligo product was used for assembly (oligo anneal and extension) and not quantified or diluted. In these cases, 3 μL of product was used in the reaction. All reactions were completed in a thermocycler (Table 4), and either immediately used in a transformation, or stored at -20°C for later use. All reagents were purchased from New England Biolabs (https://www.neb.com/).

Table 3. Single Assembly Reaction (10 µL).

Volume	Level 0, Level 2	Level 1
1.0 µL	Each insert (15 fmol)	
1.0 µL	Destination Vector (7.5 fmol)	
0.5 µL	T4 DNA Ligase (catalog no. M0202L)	
0.5 µL	SapI (catalog no. R0569L)	BsaI (catalog no. R0535L)
1.0 µL	Cut Smart w/ 1 mM ATP (catalog no. P0756S)	T4 DNA Ligase Buffer (catalog no. M0202L)
~ µL	diH2O to 10 µL	

Setup for a single assembly reaction.

Table 4. Assembly Reaction Protocol.

Step	Temperature	Time	Cycles
1	37°C	1.5 min	Level 0: 10 cycles Level 1: 20 cycles Level 2: 25 cycles
2	16°C	3 min	
3	50°C	5 min	
4	80°C	10 min	
5	4°C	Hold	

Thermocycler settings for assembly reactions. Cycles were increased depending on type of assembly.

Strains and Transformations

DNA, as whole plasmid or assembly ligations, was transformed into *Escherichia coli* DH5α chemically competent cells (Thermo Fisher, catalog no. 18265017) or *Escherichia coli* NEB 10β chemically competent cells (originally purchased from NEB; competent cells prepared in lab). All toehold test constructs were transformed into DH5α cells to ensure all measurement experiments used the same strain. Transformations followed a modified iGEM transformation protocol (Transformation, 2017). Competent cells were thawed on ice, and aliquoted into microcentrifuge tubes (50 µL aliquots for low efficiency cells as defined as ~1 x 10^6 CFU/ng DNA, 20 µL for high efficiency cells as defined as ~1 x 10^8 CFU/ng DNA). Competent cells were transformed with 1-3 µL of DNA (whole plasmid, assembly reaction, etc) and incubated on ice for 30 minutes. Transformations were heat shocked for 1 minute at 42°C, and then returned to rest on ice for 5 minutes. 900 µL of SOC media was added to each transformation, and tubes were then incubated for 1 hour in a shaker incubator at 37°C at 300 rpm. Transformations were plated on selective LB agar as a 100 µL plating and a concentrated 800 µL plating, which was spun down at 4000 rpm for 2 minutes. Selective LB agar and LB broth contained either chloramphenicol at a final concentration of 35 µg/mL for pSB1C3 and pSB3C5 based vectors or kanamycin at a final concentration of 35 µg/mL for pSB1K3 based vectors.

Cell Cultures & Glycerol Stocks

For the preparation of glycerol stocks and plasmid extraction, single colonies from transformation plates or streaked plates on selective LB agar from glycerol stocks were used to inoculate 5 mL of selective LB broth. Cultures were incubated overnight

(14-16 hours) in a shaker incubator at 37°C at 300 rpm. For each cell culture, 400 µL was removed, mixed with 200 µL of 80% glycerol, and frozen at -80°C to create a glycerol stock. The remaining culture was spun down to pellet, and plasmid was isolated with Qiagen Miniprep Skin kits (catalog no. 27106) following the vendor's protocol. Plasmid DNA concentration was quantified via a Nanodrop.

Sequencing

Part samples were verified by sequencing through Genewiz (https://www.genewiz.com), following their sanger sequencing submission guidelines. VF2 (5' TGCCACCTGACGTCTAAGAA 3') and VR (5' ATTACCGCCTTTGAGTGAGC 3') primers were used for sequencing as these priming sites are located on the pSB series plasmid backbones. Sequence files (.ab1) were uploaded to Benchling for alignment and verification. For new parts and assembly vectors, multiple colonies were often prepared for sequencing. Any incorrect part samples were disposed of.

Calibrants & Standard Curves

In order to obtain reliable and replicable measurements of test constructs, standard calibrants were tested, and then used prior to each plate reader measurement. This study used standard calibrants provided in the 2019 iGEM Measurement Kit, fluorescein and silica microspheres, and a modified version of the 2018 iGEM Interlab protocol (iGEM 2018 InterLab, 2018). Additionally, rhodamine B (Sigma-Aldrich, catalog no. 79754-25MG) was used as a calibrant for measuring red fluorescence. Fluorescein and rhodamine B were resuspended with diH_2O and 95% Ethanol, respectively, to achieve a

stock solution concentration of 100 μM. 1:10 dilutions of both fluorescent calibrants were then prepared to achieve a working solution concentration 10 μM.

All three calibrants were prepared on the same black, clear flat bottom 96 well plate (Corning, catalog no 3631) prior to plate reading. Changes to the protocol for this research included: repeating calibrants in triplicate along columns, with well A containing undiluted solution, and wells B through G containing progressive serially dilutions of 1:10, into diH2O or 95% Ethanol, depending on the calibrant (iGEM 2018 InterLab, 2018). Calibrants were run on the BioTek Synergy HT plate reader, with several filter settings used to determine best fit for measuring calibrant fluorescence (Table 5). The settings were selected based on the properties of the calibrants and fluorescent reporter proteins to be tested.

Table 5. Plate Reader Settings.

Read	**Excitation**	**Emission**	**Gain**
Absorbance (600nm)	na	na	na
Fluorescence: Filter Setting 1	485/20	528/20	55
Fluorescence: Filter Setting 2	530/25	590/35	40
Fluorescence: Filter Setting 3	530/25	590/35	45
Fluorescence: Filter Setting 4	530/25	645/40	35
Fluorescence: Filter Setting 5	360/40	460/40	40

The above settings were used on the BioTek Synergy HT plate reader for measuring calibrants and all tested constructs.

Plate Reader Measurements

The following protocol is a modified version of the 2018 iGEM Interlab protocol (iGEM 2018 InterLab, 2018). Plate reader experiments were repeated twice across two different days, and prior to each experiment a calibration and standard curve protocol was also conducted (see above).

On Day 1, samples of test constructs, including positive and negative controls, were streaked out from glycerol stocks onto LB agar plates with the appropriate antibiotic (kanamycin 35 mg/ml). 14 test constructs per fluorescent reporter were tested, along with an RFP control (BBa_J04450 in pSB1K01) and a negative control (Spacer 36INS2 in pSB1K01). Plates were incubated overnight at 37°C.

On Day 2, single colonies of test constructs were picked in triplicate (three biological replicates), and used to inoculate two 96 well cell culture plates with 1.5 mL selective LB broth per well for overnight growth. Both 96 well plates were incubated in a shaker incubator at 37°C, 980 rpm.

On Day 3, optical density measurements at OD_{600} were taken of the overnight growth plates (14-16 hrs) in the plate reader at a 1:10 dilution (10 µL cell culture into 90 µL LB kanamycin broth). New 96 well culture plates were inoculated to normalize cultures to an OD_{600} of 0.02 in a total of 1.8 mL selective LB Broth per well. OD_{600} and fluorescence measurements were taken at 0 hr, 3 hr, 6 hr, and 23 hr timepoints. Cell culture plates were removed from the shaker incubator at the specified timepoints. For each cell culture plate, three black, clear flat bottom 96 well plates were prepared (6 total) for a 1:2 dilution of culture (50 µL of culture mixed with 50 µL of selective LB broth) to establish three technical replicates per a biological replicate. Cell culture plates

were returned to the shaker incubator. Fluorescence was measured on the BioTek Synergy HT plate reader, with several filter settings used to accommodate the excitation and emission differences between reporter proteins (Table 5).

Data Conversion and Statistical Analysis

Prior to statistical analysis, raw fluorescence measurements were converted from arbitrary units (a. u.) to molecules of equivalent fluorescein (MEFL) or molecules of equivalent rhodamine (MERH) per particle. Fluorescence and absorption at OD_{600} of LB media (kanamycin) blanks were subtracted from the raw fluorescence and absorption data of tested constructs to establish net fluorescence and net absorption per replicate. This data was then multiplied by 2, due to the initial dilution factor (1:2) of cell culture used in the plate reader.

A corrected version of the 2018 iGEM Interlab Study protocol excel sheet was used to take standard calibrant data and calculate the conversion factor for MEFL (or MERH) per arbitrary unit (a.u) and silica particles per absorption at OD_{600}. Dividing these numbers, respectively, established MEFL (or MERH) per particle. For each replicate, net fluorescence was divided by net absorption, and multiplied by the conversion factor (iGEM 2018 InterLab, 2018).

For linear graphs, replicates of constructs were averaged with error bars representing standard deviation. For boxplots, all replicates are represented per construct, with error bars representing standard deviation.

Chapter III.

Results

Universal Acceptor Plasmid

pSB1C00, the Universal Acceptor Plasmid, was designed in order to create new Level 0 part samples in Type IIS format in a flexible and simple manner. pSB1C00 was built upon the pSB1C3 plasmid backbone and used the EcoRI and PstI recognition sites on pSB1C3 to ligate in the required Type IIS Level 0 cloning site and BBa_J04450 (RFP generator device) as a selection insert. Sequencing verified that pSB1C00 was successfully created and had the correct Level 0 cloning site and BBa_J04450 as its selection insert.

All new Level 0 part samples used in this research were ligated and maintained in pSB1C00, in a one-pot digest and ligation reaction with SapI. Level 0 ligations into pSB1C00 were successful, with few ligation failures and none that were attributed to pSB1C00. When Level 0 parts are assembled into this plasmid, BBa_J04450 was used to select against correct transformants.

Assembly Plasmids

Level 1 and Level 2 Type IIS assembly vectors were constructed by ligating the cloning sites of the pOdd and pEven Loop vectors, respectively, with BBa_J04450, into BioBrick plasmids using their EcoRI and PstI recognition sites. Sequencing confirmed correct Type IIS Loop cloning sites and BBa_J04450 in samples of both sets of assembly vectors (Table 6).

Sequencing of constructs showed that Level 1 assemblies into pSB1K0X vectors were successful, with few ligation failures, while Level 2 assemblies into pSB3C0X were less successful, with several ligation failures (see below for details).

Table 6. Type IIS Assembly Vectors.

Assembly Vector	**Loop Analogue**	**Built-on**	**Resistance**	**Copy**	**Selection Insert**
pSB1C00	na	pSB1C3	Chloramphenicol	High	BBa_J04450
pSB1K01	pOdd1	pSB1K3	Kanamycin	High	BBa_J04450
pSB1K02	pOdd2	pSB1K3	Kanamycin	High	BBa_J04450
pSB1K03	pOdd3	pSB1K3	Kanamycin	High	BBa_J04450
pSB1K04	pOdd4	pSB1K3	Kanamycin	High	BBa_J04450
pSB3C01	pEven1	pSB3C5	Chloramphenicol	Medium	BBa_J04450
pSB3C02	pEven2	pSB3C5	Chloramphenicol	Medium	BBa_J04450
pSB3C03	pEven3	pSB3C5	Chloramphenicol	Medium	BBa_J04450
pSB3C04	pEven4	pSB3C5	Chloramphenicol	Medium	BBa_J04450

The listed Type IIS vectors were made to create new basic parts (pSB1C00), assemble transcriptional units (pSB1K01-04), and multi-transcriptional units (pSB3C01-04). All vectors cloning sites and selection inserts were sequence confirmed. (Pollack et al., 2018).

Terminator

While BBa_B0015, the most used transcriptional terminator in iGEM's Registry, has a few samples in Type IIS format, due to differing fusion sites or inconsistent sequencing results, a new sample of BBa_B0015 was made and sequence verified for this research ("BBa_B0015," 2003). For the purposes of this research, a single terminator sufficed, but ideally, additional terminators should be made in Type IIS format.

Reporter Proteins

Several reporter proteins in Type IIS format were made and sequence verified for this research (Table 7). Samples of these reporter proteins existed in the Registry but required the addition of fusion sites and, in some cases, minor modifications, including site mutagenesis and addition of stop codons. The primary focus was on fluorescent proteins, as these would be used to measure output of the translational modifications of toehold switches in a plate reader.

Of the six fluorescent proteins made, four (EiraCFP, JuniperGFP, TannenRFP, and BlazeYFP) were used in the plate reader experiments. Chromoproteins were also made in Type IIS format, as these are useful when making observations under visible light. With the exception of a few chromoproteins, all reporter proteins were successfully PCRed, inserted into pSB1C00, and sequence verified. The following parts were attempted, but not successfully cloned: AeBlue, amilCP, amilGFP, cjBlue, and fwYellow.

Table 7. Type IIS Reporter Proteins.

Name	NickName	Template	Excitation	Emission
EiraCFP	CFP 1	BBa_J97000	398	498
eCFP	CFP 2	BBa_E0020	439	476
JuniperGFP	GFP 1	BBa_J97001	508	521
TannenRFP	RFP 1	BBa_J97003	550	565
DsRed	RFP 2	BBa_K1323009		
BlazeYFP	YFP 1	BBa_J97002	515	534
eYFP	YFP 2	BBa_E0030	514	527
amajLime		BBa_K1033916		
asPink		BBa_K1033933		
eforRed		BBa_K592012		
gfasPurple		BBa_K1033919		
spisPink		BBa_K1033932		
tsPurple		BBa_K1033906		

The listed reporter proteins had samples made in Type IIS format and inserted into the pSB1C00. Their original sample template was acquired from the iGEM Registry (http://www.parts.igem.org). All new part samples were sequence confirmed.

Toehold Switches

Of the fifteen toehold switches initially designed, eleven were constructed in lab, along with one control toehold switch (Table 9). As completely new parts, toehold switch samples were made with oligo annealing and extension, followed by an assembly reaction into pSB1C00, and transformation. More than 90% of transformants appeared to be successful through red/white screening, and all toehold switches were confirmed through sequencing.

Spacers

Only two transcriptional units, the toehold constructs and target mRNA constructs, were used for multi-transcriptional constructs (Level 2s). However, for Loop assembly, exactly four transcriptional units (Level 1s) are needed to complete a Level 2 assembly into destination vectors (Figure 6b). Spacers were used to fill in as non-transcribed Level 1 parts in order to complete Level 2 assembles. Four 36 base pair spacers (Table 10) were made with oligo annealing, followed by insertion into pSB1K0X assembly vectors, transformation, and sequencing for verification.

Transformants for correct spacers was very low, resulting in not all desired spacer and assembly vector combinations. Observations from red/white screening showed that the majority of transformants contained the selection marker (BBa_J04450), and few, if any colonies were white (Spacer). This was an unexpected result, as all toehold switches were made with the same protocol, with much greater success. However, all spacers required for Level 2 assemblies were confirmed through sequencing (Table 12).

Level 1 Constructs

93 Level 1 constructs were assembled for this research. The majority of these were toehold constructs, toehold switches paired with fluorescent reporter proteins, and target mRNA constructs, weak translational control elements paired with fluorescent reporter proteins (Table 13). Initial testing of Type IIS assemblies and new parts resulted in new constructs that were not useful for the subsequent characterization experiments, and have been omitted as a result: these included expression constructs with chromoprotein reporters, and additional combinations of promoters and BCDs. Level 1

assemblies into the pSB1K0X vectors were successful. More than 90% of transformants appeared to be correct through red/white screening, with sequencing confirming them. It should be noted that the selection marker, BBa_J04450, is an RFP expression device. This may cause issues when similar RFPs and devices are assembled into pSB1K01-04, but can be remedied with alternative selection markers.

Level 2 Constructs

The Level 2 constructs assembled for this study were multi-transcriptional units that include a toehold construct and a target mRNA construct with spacers in between them. Level 2 assemblies into pSB3C0X were less successful than all other assemblies, with several ligation failures even when multiple colonies were selected for sequencing. From an initial test of 17 different Level 2 assemblies, only 8 were sequence confirmed (Table 14). This presented a major limitation to characterizing the toehold switches completely, as these Level 2 constructs were needed to test their specificity and orthogonality.

Calibrants and Standard Curves

This study used standard calibrants, specifically fluorescein and silica microspheres, laid out in the 2018 Interlab study, with the addition of Rhodamine B, as a calibrant for measuring red fluorescence (iGEM 2018 InterLab, 2018). Both fluorescent standards were run against the plate reader settings in Table 5. Of the 5 filter settings, fluorescein was best detected at setting 1 (excitation: 485/20, emission: 528/20, gain: 55) and rhodamine was best detected at setting 3 (excitation: 530/25, emission: 590/35, gain:

45). Prior testing had shown that these two settings were also best at characterizing three out of four reporter proteins (see below for details).

While plate reader settings were not changed for both plate reader experiments, the calibrants were used before each experiment to account for any environmental changes or errors. The results of these calibrants were graphed as standard curves (Fig ures 9, 10, 11). These were used to both validate the plate reader settings for the fluorescent reporter proteins, and to create a conversion for arbitrary units (a.u) to MEFL, molecules of equivalent fluorescein, or MERH, molecules of equivalent rhodamine, to ensure that fluorescence results would have comparable units (Table 15).

Fluorescent Reporter Protein Characterization

Four ip-free fluorescent reporter proteins (EiraCFP, JuniperGFP, TannenRFP, and BlazeYFP) were characterized by measuring their fluorescence in a plate reader. These reporter proteins were paired with well-characterized promoters and ribosome binding sites (Table 8) in order to validate their expression and their use in toehold switch constructs. All fluorescent reporter proteins were measured using the plate reader settings designated in Table 5.

While not a focus of this research, this data is useful for future applications and for initial characterization of the reporter proteins in this collection. Ideally, it would be further expanded upon with additional timepoints, adjustments to filter settings, and transcription/translation control elements.

Table 8. Well-characterized promoters and ribosome binding sites.

Promoter	**Transcription**	**RBS / 5' UTR**	**Translation**
BBa_J23100	High	Bba_B0034	High
Bba_J23106	Medium-High	Bba_B0034	High
Bba_J23100	High	BNonTS	Unknown
Bba_J23100	High	BCD8 (Bba_K1114108)	Low
Bba_J23106	Medium-High	BCD8 (Bba_K1114108)	Low

All four reporter proteins were paired with these well-characterized promoters to create expression devices with some predictability. BNonTS contains partial sequences from the toehold design template, and its translation control is unknown.

EiraCFP

EiraCFP (BBa_J97000) has a documented excitation of 398 nm and an emission of 498 nm ("BBa_J97000," 2014). Of the five filter settings used for the plate reader measurements, only filter setting 5 (Excitation: 360/40, Emission: 460/40, Gain: 40) was close to the required excitation and emission. However, this setting was not sufficient to obtain measurements of fluorescence as both excitation and emission were still out of range. EiraCFP, measured at filter setting 1, did not show detectable fluorescence when compared to negative controls, at 6 or 23 hr timepoints (Figure 1). As such, EiraCFP could not be characterized on the plate reader. The data of toehold constructs paired with EiraCFP is not useful and has been omitted from further analysis.

Potential future work should entail finding a fluorescent standard for calibrating measurements of cyan fluorescent proteins and using a different plate reader with a wider range of filter settings. Other cyan fluorescent proteins with more suitable excitation/emission should also be considered.

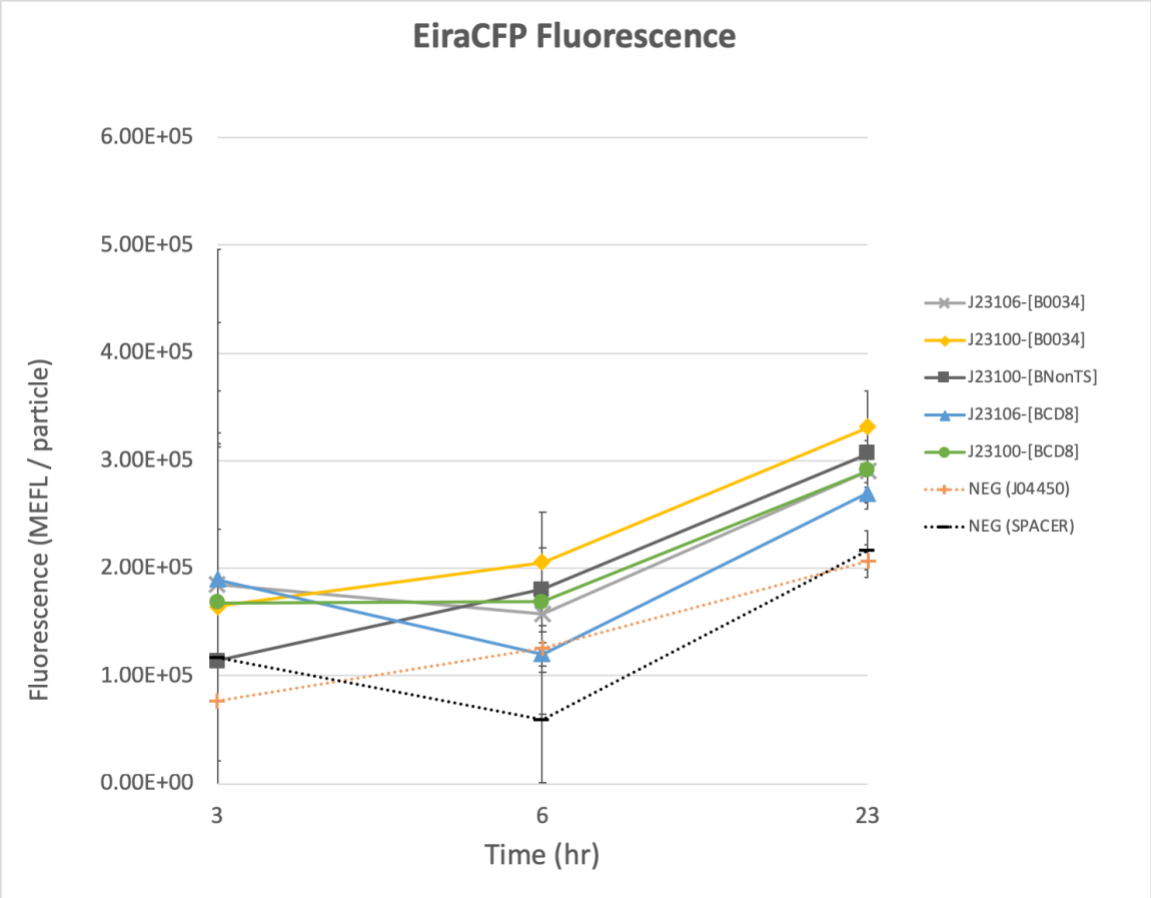

Figure 1. EiraCFP characterization.

Fluorescence (a.u) and absorption collected using filter setting 1 on Table 5 at the following timepoints (0 hr excluded) and converted to MEFL per particle. Data from both plate reader experiments is represented as average ±SD. n=18 per datapoint.

JuniperGFP

JuniperGFP (BBa_J97001) has an excitation of 508 nm and an emission of 521 nm, and its fluorescence was easily measured using filter setting 1 (excitation: 485/20, emission: 528/20, gain: 55) ("BBa_J97001," 2014). The following data demonstrates that JuniperGFP is suitable as a fluorescent reporter protein, as several of the tested constructs exhibited increased fluorescence over time in comparison to the negative controls (Figure 2).

However, the control toehold, BNonTS, did not show increased fluorescence when compared to the negative controls. This may mean that the whole or partial sequence of BNonTS is inhibiting translation of JuniperGFP. Since BNonTS contains the same RBS and linker sequence as all of the toeholds, it cannot be excluded that those sequences are unintentionally interfering with translation when any toehold switch is paired with JuniperGFP.

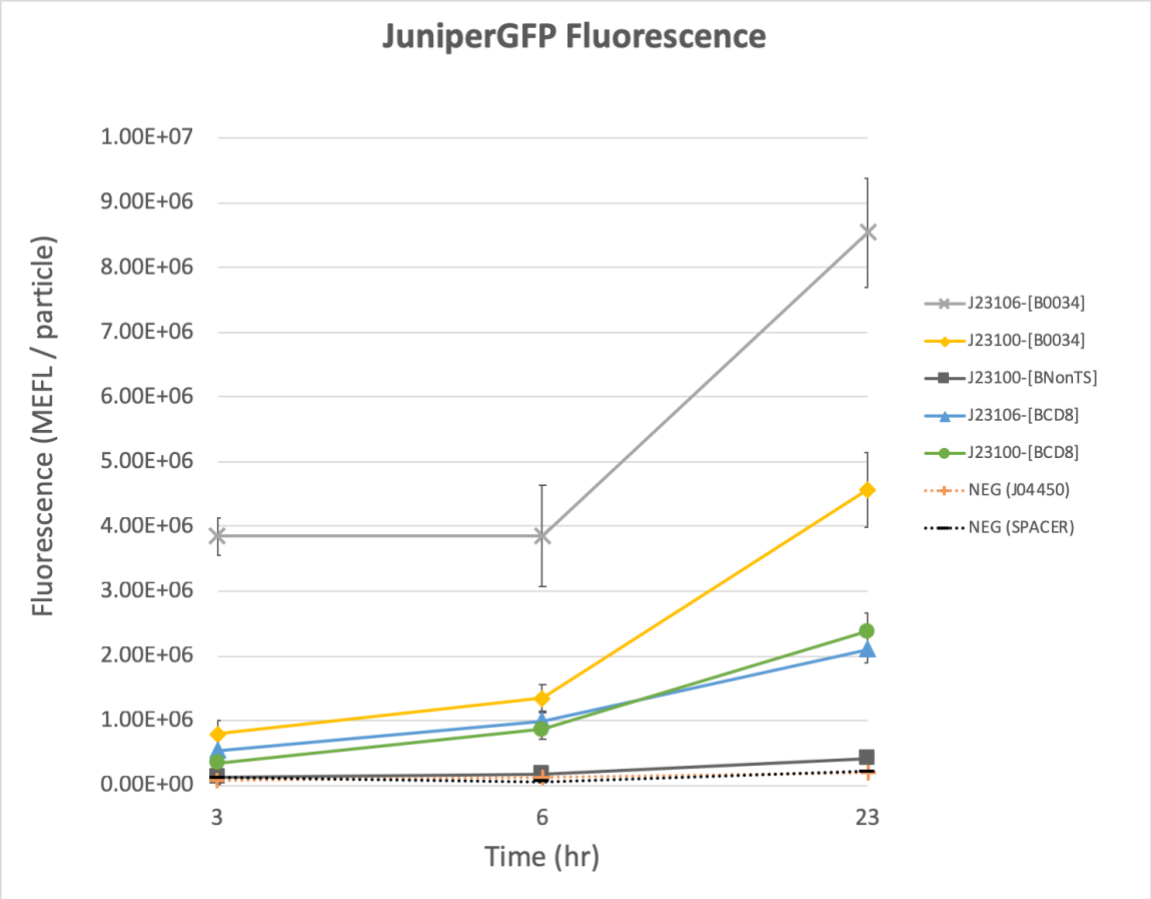

Figure 2. JuniperGFP characterization.

Fluorescence (a.u) and absorption collected using filter setting 1 on Table 5 at the following timepoints (0 hr excluded) and converted to MEFL per particle. Data from both plate reader experiments is represented as average ±SD. n=18 per datapoint.

TannenRFP

TannenRFP (BBa_J97003) has a documented excitation of 550 nm and an emission of 565 nm and a medium maturation rate ("BBa_J97003," 2014). Filter setting 3 was best at capturing its fluorescence (excitation: 530/25, emission: 590/35, gain: 45). While BNonTS, the control toehold, did not match fluorescence with the highest expressing constructs (J23106-B0034 and J23100-B0034), it did allow for expression higher than the low expression construct (J23106-BCD8) (Figure 3). Interestingly, the J23100-BCD8 constructs appears to have no effect on fluorescence when compared to the negative control.

The fluorescence data demonstrates that TannenRFP is useful as a reporter protein with two caveats. Firstly, TannenRFP's medium maturation rate may be an issue for some genetic circuit designs. This is evident when comparing its 6 hr and 23 hr timepoints to the positive control, BBa_J04450, which appears to use a faster maturing RFP ("BBa_E1010," 2004) (Figure 3). As a result, the 6 hr timepoint for toehold constructs containing TannenRFP will not be as useful as the 23 hr timepoint. Secondly, due to the narrow gap between TannenRFP's excitation and emission, its fluorescence may not be well represented with the available plate reader settings.

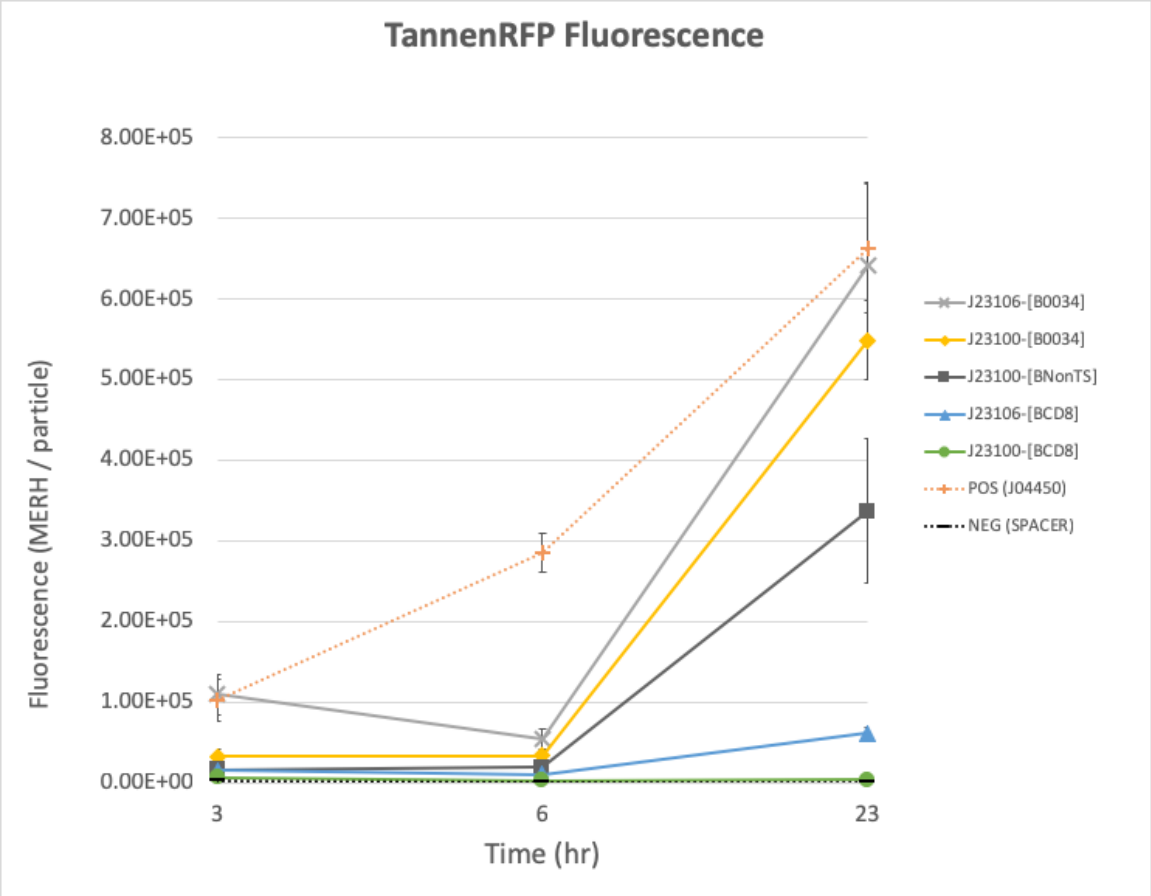

Figure 3. TannenRFP characterization.

Fluorescence (a.u) and absorption collected using filter setting 1 on Table 5 at the following timepoints (0 hr excluded) and converted to MERH per particle. Data from both plate reader experiments is represented as average ±SD. n=18 per datapoint

BlazeYFP

BlazeYFP (BBa_J97002) has a documented excitation of 515 nm and an emission of 534 nm ("BBa_J97002," 2014). BlazeYFP is shown to work well as a fluorescent reporter protein, as all tested constructs exhibited significant fluorescence over time in comparison to the negative controls with filter setting 1 (excitation: 485/20, emission:

528/20, gain: 55) (Figure 4). Notably, BNonTS, the control toehold, allowed for fluorescence expression close to that of the highest expressing construct (J23106-B0034).

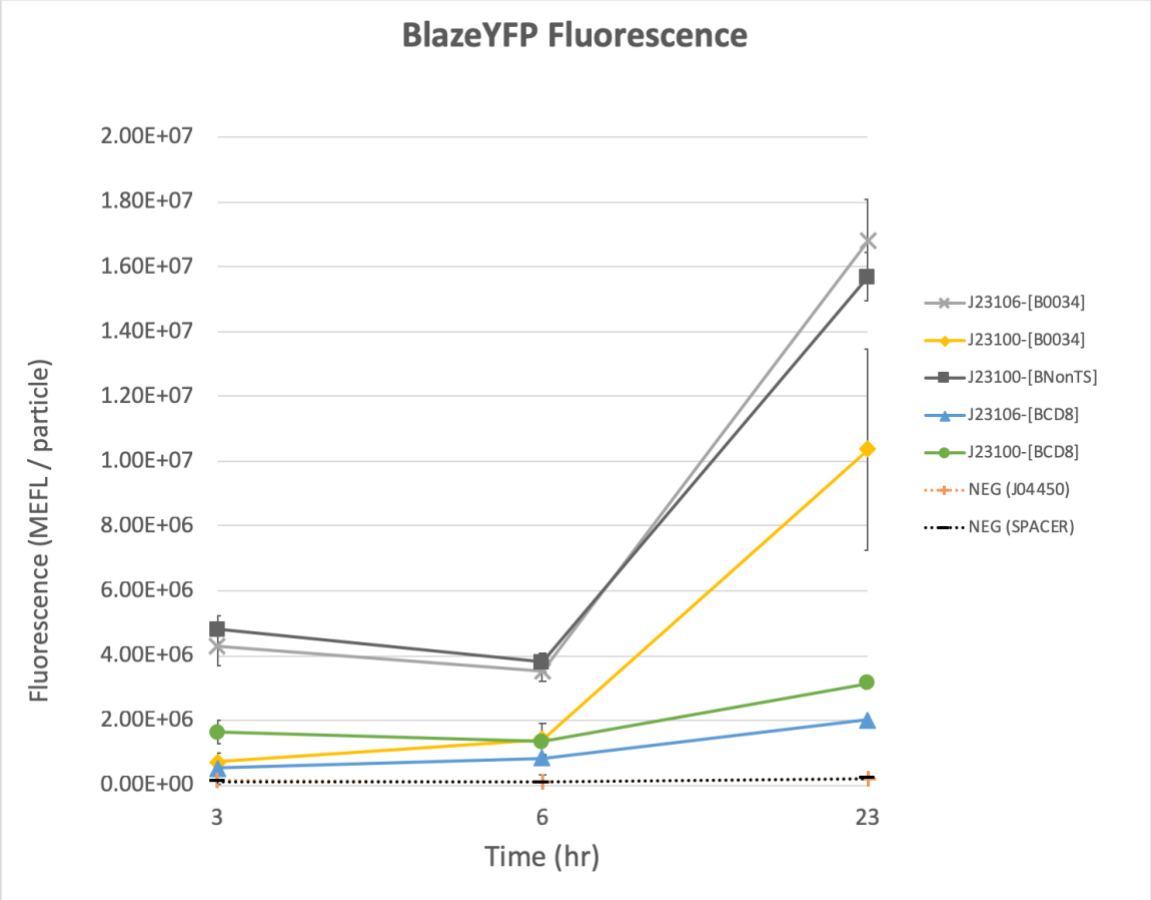

Figure 4. BlazeYFP characterization.

Fluorescence (a.u) and absorption collected using filter setting 1 on Table 5 at the following timepoints (0 hr excluded) and converted to MEFL per particle. Data from both plate reader experiments is represented as average ±SD. n=18 per datapoint.

Toehold Switches and JuniperGFP

None of the toehold switches tested allowed for significant JuniperGFP expression, even in comparison to the low expression positive controls, BCD8s (Figure 12). This may mean that their hairpin structure is working as desired and preventing translation by sequestering the ribosome binding site. Although, YFP1-TS2 did show some expression in comparison to the negative control, and is likely leaky. Of the three toehold switches designed to be triggered by JuniperGFP (GFP1-TS1, GFP1-TS2, and GFP1-TS3), none exhibited significant expression when compared to the negative control. This may demonstrate that these toehold switches do not work as expected; they are not triggered by the mRNA strand copies of JuniperGFP in the cell.

Notably, the control switch (BNonTS) also did not allow for significant expression, even though it was designed to lack a hairpin structure (Figure 12). As noted before, this may mean that the RBS and linker sequence of BNonTS, and all other toeholds, is unintentionally inhibiting translation of JuniperGFP.

Toehold Switches and TannenRFP

While eight of the toehold switch constructs did not fluoresce, two toehold switches, CFP1-TS1 and YFP1-TS2, allowed for TannenRFP expression close to that of the low expression positive control, J23106-BCD8 (Figure 13). For the former, this may mean that their hairpin structure is working as desired and preventing translation, while CFP1-TS1 and YFP1-TS2 may be leaky toeholds. Of the two toehold switches designed to be triggered by TannenRFP (RFP1-TS1 and RFP1-TS2), neither exhibited increased expression when compared to the negative control. This may demonstrate that these toehold switches do not work as they have not “self-triggered” on the mRNA strands of

TannenRFP in the cell. When triggered by their target mRNA it would be expected that these toehold switches allow for fluorescence expression somewhere between the range of BNonTS, the control toehold, and the low expression control (J23106-BCD8).

Toehold Switches and BlazeYFP

Toehold switches paired with BlazeYFP showed the most variability in fluorescence expression and by extension, translation leakiness (Figure 14). RFP1-TS1, RFP1-TS2, and GFP1-TS3 constructs did not fluoresce compared to the negative control. GFP1-TS1, CFP1-TS2 showed detectable fluorescence over the negative control. GFP1-TS2, YFP1-TS1, CFP1-TS1, and YFP1-TS2 allowed for BlazeYFP expression, close to that or exceeding the low expression positive controls, (J23106-BCD8 and J23100-BCD8).

Both toehold switches (YFP1-TS1 and YFP1-TS2) designed to be triggered by BlazeYFP exhibited increased expression when compared to the negative control and low expression positive controls (Figure 14). This may demonstrate that these toehold switches are working if they are being triggered by the BlazeYFP mRNA strands in the cell. However, as noted before, when paired with JuniperGFP (Figure 12) and TannenRFP (Figure 13), YFP1-TS2 had also been shown to allow for fluorescence expression.

Chapter IV.

Discussion

Significance of Results

Type IIS assembly methods, like MoClo, have been shown to be a useful tool for synthetic biologists, allowing efficient one-pot assembly of multiple biological parts in order to create genetic circuits quickly and reliably (Weber et al., 2011). The proliferation of Type IIS assembly has led to the creation of several assembly standards, like CIDAR MoClo, PhytoBricks, and Loop, along with collections of parts that adhere to these standards (Iverson et al., 2016; Patron et al., 2015; Pollack et al., 2018). However, building up libraries for these assembly standards is an ongoing activity, and there is always room for new well-characterized parts and samples.

Several new Type IIS parts samples and assembly vectors were created and sequence confirmed for this research: 13 reporter proteins, 11 toehold switches, 1 terminator, and 9 assembly vectors. Creation of new basic part samples through PCR or oligo annealing and extension worked well, with few issues. Correct transformants cloned into pSB1C00 were easily selected through red/white screening, and sequencing confirmed them. This demonstrated the efficacy and usefulness of the Universal Acceptor Plasmid and protocol in creating new Level 0 basic parts.

Paired with already existing Type IIS parts (Table 11), the new basic parts generated in this study were used to assemble 93 different transcriptional units into the pSB1K01-04 assembly vectors. These assemblies were quick and reliable, with over 90%

of transformants appearing to be correct through red/white screening, and sequencing confirming them. These results are consistent with other Type IIS assembly methods (Iverson et al., 2016; Pollack et al., 2018). One area for improvement would be to use additional selection markers, like *lacZ*, for pSB1K01-04, to accommodate different screening techniques and requirements.

The Level 2 assembly vectors, pSB3C01-04, proved to be the major limitation of this study (Table 14). While eight multi-transcriptional units were successful assembled, there were several ligation failures or incorrect transformants selected. Issues with the cloning site of pSB3C01-04, and by extension Loop assembly, are unlikely, as Level 2 assemblies have been shown to be greater than 80% efficient (Pollack et al., 2018). There are a few different options that could be addressed in the future, to troubleshoot or develop a better Level 2 assembly vector.

Firstly, while the cloning sites and selection markers on pSB3C01-04 were sequence verified, the whole plasmid was not. Whole plasmid sequencing may uncover discrepancies between the plasmid sample and its documented sequence that may be causing assembly issues. Secondly, toehold switch constructs and target mRNA constructs may have been too taxing on cells, due to a combination of the constructs using strong constitutive promoters, BBa_J23100 and BBa_J23106, respectively, and pSB3C01-04 being a low-medium copy plasmid. A simple solution to fix this assembly issue may be to obtain the well-characterized Loop Assembly Vectors that are currently available under the OpenMTA (Pollack et al., 2018).

Characterization work on constructs was successful, due in large part to the use of an adapted 2018 Interlab protocol (iGEM 2018 InterLab, 2018). The use of calibrants and process controls were immensely important, both in validating the experimental protocol and also in providing fluorescence measurements in comparable units. Four fluorescent reporter proteins were tested in the plate reader experiments, with three, JuniperGFP, TannenRFP, and BlazeYFP, showing useful initial characterization data (Figures 2, 3, 4). These results can be further expanded upon by collecting data at additional timepoints, and by assembling constructs with a greater variety of transcriptional and translational control elements. The lack of usable data for EiraCFP demonstrates that it may be an unsuitable cyan fluorescent reporter for some plate readers (Figure 1).

Samples of eleven toeholds were created and sequence confirmed, with nine of them characterized alongside downstream fluorescent reporters to observe translation leakiness. While many of the toehold switches appear to be inhibiting translation of their downstream reporter protein (Figures 12, 13, 14), it cannot be confirmed that they are actually working. A number of issues arose that would require troubleshooting.

A more suitable control would be required, as BNonTS had greatly varying effects on expression depending on the fluorescent reporter protein it was paired with (Figures 2, 3, 4). Toehold switches that were paired with their respective trigger mRNA also did not show any increased expression when compared to other pairwise combinations, with the exception of YFP-TS1 (Figure 14). While this may mean that self-triggering of toehold switches is not possible or inhibitory, it's also possible that the toehold switches are not working as expected. Additional characterization work that could help address these questions was limited by issues with Level 2 assemblies into

pSB3C0X vectors. The eight multi-transcriptional that were assembled and sequence confirmed were not sufficient to test toehold switch specificity and orthogonality.

It was hypothesized that a set of standardized toehold switches could be developed with high specificity and orthogonality to only express a downstream reporter protein in response to a trigger mRNA sequence. The data generated from the toehold switch constructs is not sufficient for testing this hypothesis, however, this study has provided the initial infrastructure for such work in the future. New Type IIS toehold switch parts can be made using the Universal Acceptor Vector. These can be assembled into Level 1 assembly vectors with a variety of reporter proteins. This Type IIS library will be open to sharing and expansion; the parts created for this research will be added and documented on the iGEM Registry, and made available to all users, while new parts and assembly vectors can be added at any time.

Study Limitations

While the iGEM Registry has many samples, access to DNA synthesis would have allowed for more part samples, including toehold switches and reporter proteins, to be added to this Type IIS library. This research relied on pre-existing samples and their modification through PCR, and the creation of entirely new sequences by oligo annealing and extension. While this worked well, it did limit experimental design, as a wider range of fluorescent reporters and toehold switches may have been helpful.

The BioTek Synergy HT plate reader used in this study also had limitations due to its range of filter settings. In particular, the cyan fluorescent reporter, EiraCFP, could not be characterized on the plate reader because a filter setting for its specific excitation and emission were not available (Figure 1). While all constructs containing EiraCFP were

successfully assembled (Table 13), this meant that none of them provided usable characterization data.

Lastly, a major limitation for toehold switch testing and characterization was the low rate of success for multi-transcriptional unit assemblies into the Level 2 assembly vectors, pSB3C01-04 (Table 14). This prevented characterization of toehold switch orthogonality, as toehold switch constructs were not paired with their respective target mRNA, or potential mistargets.

Future Directions

The results of this study can be built upon while also addressing some of the limitations. The Type IIS library created for this study should be expanded upon. In particular, generating more Level 0 basic part samples would be useful. One way to address physical limitations such as the filter settings available on a plate readers is to have a wider variety of fluorescent reporter proteins. Online databases like fpbase (https://www.fpbase.org/), provide the sequences for many related reporter proteins, along with their differing characteristics. Having access to fluorescent reporter proteins with more suitable excitation and emission wavelengths, and maturation times would be useful.

Additionally, new toehold switches should be designed and tested for each target mRNA. New design software and research on toehold switches has provided improved design guidelines for toeholds, and a diversity of hairpin structure would be useful once ideal target sequences have been identified (To et al., 2018; Peters et al., 2018).

While the issues with the Level 2 Assembly vector should be addressed, another option would be to use co-transformation of Level 1 vectors (Green et al., 2014). This

would require creating new Level 1 Assembly vectors with an antibiotic resistance different to that of kanamycin (pSB1K01-04) and chloramphenicol (pSB1C00), and with a different replication origin as well. This would allow target mRNA constructs to be assembled into this new plasmid and then co-transformed with current toehold switch constructs, preventing the need for assembling multi-transcriptional units (Level 2s).

Conclusion

The goal of this research was to create and characterize a library of Type IIS parts that could be used to quickly and reliably build genetic circuits. Library creation was largely successful, with sequence-confirmed samples of 26 new basic parts, and nine assembly vectors generated. Over 90 Level 1 transcriptional units were built, demonstrating the effectiveness of Type IIS assembly and the potential for this library to be used to quickly assemble genetic circuits.

However, it was also hypothesized that a set of orthogonal toehold switches could be designed and characterized to respond to their cognate trigger mRNA sequences with high specificity. While prior literature has shown this to be possible, the issues with assembling multi-transcriptional constructs prevented any further testing; as such, the hypothesis could not be tested. The characterization work that was conducted, while initial, has provided useful data for three fluorescent reporter proteins and nine toehold switches. Additionally, this characterization work used a standardized measurement protocol, which offered higher precision and repeatability, and data in comparable units. Altogether, this library serves as both a proof-of-concept and a ready-to-use toolkit, allowing a synthetic biologist to quickly assemble and prototype a new genetic circuit design with reliability and some predictability.

Appendix

Table 9. Toehold Switch Sequences

Name	Sequence
CFP1-TS1	5'TACTGGGCGCGGTCTTTGCTCAGTTTGGTGTGTTTGCGTTATAGTTATGAGACAAGAACAGAGGAGACATAACATGAACGCAAACAACCTGGCGGCAGCGCAGAAAATG 3'
CFP1-TS2	5'TACTGGGTTTGGTAACCAGTTTTTCGGTCACACCTTCGTTATAGTTATGAGACAAGAACAGAGGAGACATAACATGAACGAAGGTAACCTGGCGGCAGCGCAGAAAATG 3'
CFP2-TS1	5'TACTGGGCGGCTGAAGCACTGCACGCCCCAGGTCAGGTTATAGTTATGAGACAAGAACAGAGGAGACATAACATGAACCTGACCAACCTGGCGGCAGCGCAGAAAATG 3'
GFP1-TS1	5'TACTGGGCATACGGGATTTTACCATGAAACAACAGTGGTTATAGTTATGAGACAAGAACAGAGGAGACATAACATGAACCACTGTAACCTGGCGGCAGCGCAGAAAATG 3'
GFP1-TS2	5'TACTGGGATTTGTAGAAGTCTTTCAGCCCCGGGCCATGTTATAGTTATGAGACAAGAACAGAGGAGACATAACATGAACATGGCCAACCTGGCGGCAGCGCAGAAAATG 3'
GFP1-TS3	5'TACTGGGTCCGGATCCTTACCGAAGCTCGTCCAGACGGTTATAGTTATGAGACAAGAACAGAGGAGACATAACATGAACCGTCTGAACCTGGCGGCAGCGCAGAAAATG 3'
RFP1-TS1	5'TACTGGGTCCTTATCCAGACTAATGTGCGCGCTCGCCGTTATAGTTATGAGACAAGAACAGAGGAGACATAACATGAACGGCGAGAACCTGGCGGCAGCGCAGAAAATG 3'
RFP1-TS2	5'TACTGGGACAAGCACGTGTTCGATAATGTGATTCGGCGTTATAGTTATGAGACAAGAACAGAGGAGACATAACATGAACGCCGAAAACCTGGCGGCAGCGCAGAAAATG 3'
YFP1-TS1	5'TACTGGGCTTTCTCAAACAGTTTTGCACCTTCCGTCAATGTTATAGTTATGAGACAAGAACAGAGGAGACATAACATGAACATTGACAACCTGGCGGCAGCGCAGAAAATG 3'
YFP1-TS2	5'TACTGGGTAACATCCTTGCTCAGCGTGACATGGTAGTTATAGTTATGAGACAAGAACAGAGGAGACATAACATGAACTACCATAACCTGGCGGCAGCGCAGAAAATG 3'
YFP2-TS1	5'TACTGGGGCGAAGCATTGCAGGCCGTAGCCGAAGGTTATAGTTATGAGACAAGAACAGAGGAGACATAACATGAACCTTCGGAACCTGGCGGCAGCGCAGAAAATG 3'
BNonTS	5'TACTGGGAGACAAGAACAGAGGAGACATAACATGAACCACTGTAACCTGGCGGCAGCGCAGAAAATG 3'

List of toehold switches designed for this research. The name of the toehold switch (Ex. CFP1-TS1) refers to the fluorescent reporter (CFP1) it is targeting and its target number (TS1). All toehold switches were sequence confirmed.

Table 10. Spacers Sequences

Name	**Sequence**
36INS1	5' CCTGCAGTATTCATTTTCAGCTTACGGAAGGTAGAT 3'
36INS2	5' AGCAGTTACTCAAGTGGTCAGGAGGCAGACGCAGCG 3'
36INS3	5' CCTTTTCACGAGTCGCGTACTCTCCTAACTATCAAG 3'
36INS7	5' AGGGACGACCCGCGCACAGAATGTGTCGGGGTAACA 3'

36 base pair spacers were used to fill in as non-transcribed Level 1 parts to complete Level 2 assemblies and to add space between constructs. Four spacer sequences were selected for work done by Carr et al.

Table 11. Existing Type IIS Part Samples

NickName	Part Number	Level	Part Type	Plasmid
BBa_J23100	BBa_K1114000	L0	Promoter	pSB1C3
BBa_J23106	BBa_K1114009	L0	Promoter	pSB1C3
BBa_J23116	BBa_K1114018	L0	Promoter	pSB1C3
BBa_J23117	BBa_K1114020	L0	Promoter	pSB1C3
BBa_I13453	BBa_K1114023	L0	Promoter	pSB1C3
BBa_R0040	BBa_K1114025	L0	Promoter	pSB1C3
BBa_R0063	BBa_K783024	L0	Promoter	pSB1C3
BBa_B0030	BBa_K1114100	L0	RBS	pSB1C3
BBa_B0031	BBa_K1114101	L0	RBS	pSB1C3
BBa_B0032	BBa_K1114102	L0	RBS	pSB1C3
BBa_B0033	BBa_K1114103	L0	RBS	pSB1C3
BBa_B0034	BBa_K1114104	L0	RBS	pSB1C3
BCD 2	BBa_K1114107	L0	RBS	pSB1C3
BCD 8	BBa_K1114108	L0	RBS	pSB1C3
BCD 12	BBa_K1114109	L0	RBS	pSB1C3
BCD 13	BBa_K1114110	L0	RBS	pSB1C3
BCD 16	BBa_K1114111	L0	RBS	pSB1C3

Type IIS part samples retrieved from the iGEM Registry (http://parts.igem.org) and used in this study. These parts required no further modification and were all previously sequence confirmed.

Table 12. Spacers Assembled

Spacer	**Vector**
36INS1	pSB1K02
36INS2	pSB1K02
36INS2	pSB1K03
36INS3	pSB1K04
36INS7	pSB1K04

The following table contains the spacers successfully assembled into their Level 1 assembly vector. Spacers were used to fill in as non-transcribed Level 1 parts to complete Level 2 assembles. Sequences for these 36 base pair spacers can be found on Table 10.

Table 13. Level 1 Constructs

Promoter	RBS	CDS	Terminator	Type	Nick Name
J23106	B0034	CFP1	B0015	mRNA	J23106-[B0034]-CFP1
J23106	BCD8	CFP1	B0015	mRNA	J23106-[BCD8]-CFP1
J23100	B0034	CFP1	B0015	mRNA	J23100-[B0034]-CFP1
J23100	BCD8	CFP1	B0015	mRNA	J23100-[BCD8]-CFP1
J23100	BNonTS	CFP1	B0015	Switch	J23100-[BNonTS]-CFP1
J23100	CFP1-TS1	CFP1	B0015	Switch	J23100-[CFP1-TS1]-CFP1
J23100	CFP1-TS2	CFP1	B0015	Switch	J23100-[CFP1-TS2]-CFP1
J23100	GFP1-TS1	CFP1	B0015	Switch	J23100-[GFP1-TS1]-CFP1
J23100	GFP1-TS2	CFP1	B0015	Switch	J23100-[GFP1-TS2]-CFP1
J23100	GFP1-TS3	CFP1	B0015	Switch	J23100-[GFP1-TS3]-CFP1
J23100	RFP1-TS1	CFP1	B0015	Switch	J23100-[RFP1-TS1]-CFP1
J23100	RFP1-TS2	CFP1	B0015	Switch	J23100-[RFP1-TS2]-CFP1
J23100	YFP1-TS1	CFP1	B0015	Switch	J23100-[YFP1-TS1]-CFP1
J23100	YFP1-TS2	CFP1	B0015	Switch	J23100-[YFP1-TS2]-CFP1
J23106	B0034	GFP1	B0015	mRNA	J23106-[B0034]-GFP1
J23106	BCD8	GFP1	B0015	mRNA	J23106-[BCD8]-GFP1
J23100	B0034	GFP1	B0015	mRNA	J23100-[B0034]-GFP1
J23100	BCD8	GFP1	B0015	mRNA	J23100-[BCD8]-GFP1
J23100	BNonTS	GFP1	B0015	Switch	J23100-[BNonTS]-GFP1
J23100	CFP1-TS1	GFP1	B0015	Switch	J23100-[CFP1-TS1]-GFP1
J23100	CFP1-TS2	GFP1	B0015	Switch	J23100-[CFP1-TS2]-GFP1
J23100	GFP1-TS1	GFP1	B0015	Switch	J23100-[GFP1-TS1]-GFP1
J23100	GFP1-TS2	GFP1	B0015	Switch	J23100-[GFP1-TS2]-GFP1
J23100	GFP1-TS3	GFP1	B0015	Switch	J23100-[GFP1-TS3]-GFP1
J23100	RFP1-TS1	GFP1	B0015	Switch	J23100-[RFP1-TS1]-GFP1
J23100	RFP1-TS2	GFP1	B0015	Switch	J23100-[RFP1-TS2]-GFP1
J23100	YFP1-TS1	GFP1	B0015	Switch	J23100-[YFP1-TS1]-GFP1
J23100	YFP1-TS2	GFP1	B0015	Switch	J23100-[YFP1-TS2]-GFP1
J23106	B0034	RFP1	B0015	mRNA	J23106-[B0034]-RFP1

J23106	BCD8	RFP1	B0015	mRNA	J23106-[BCD8]-RFP1
J23100	B0034	RFP1	B0015	mRNA	J23100-[B0034]-RFP1
J23100	BCD8	RFP1	B0015	mRNA	J23100-[BCD8]-RFP1
J23100	BNonTS	RFP1	B0015	Switch	J23100-[BNonTS]-RFP1
J23100	CFP1-TS1	RFP1	B0015	Switch	J23100-[CFP1-TS1]-RFP1
J23100	CFP1-TS2	RFP1	B0015	Switch	J23100-[CFP1-TS2]-RFP1
J23100	GFP1-TS1	RFP1	B0015	Switch	J23100-[GFP1-TS1]-RFP1
J23100	GFP1-TS2	RFP1	B0015	Switch	J23100-[GFP1-TS2]-RFP1
J23100	GFP1-TS3	RFP1	B0015	Switch	J23100-[GFP1-TS3]-RFP1
J23100	RFP1-TS1	RFP1	B0015	Switch	J23100-[RFP1-TS1]-RFP1
J23100	RFP1-TS2	RFP1	B0015	Switch	J23100-[RFP1-TS2]-RFP1
J23100	YFP1-TS1	RFP1	B0015	Switch	J23100-[YFP1-TS1]-RFP1
J23100	YFP1-TS2	RFP1	B0015	Switch	J23100-[YFP1-TS2]-RFP1
J23106	B0034	YFP1	B0015	mRNA	J23106-[B0034]-YFP1
J23106	BCD8	YFP1	B0015	mRNA	J23106-[BCD8]-YFP1
J23100	B0034	YFP1	B0015	mRNA	J23100-[B0034]-YFP1
J23100	BCD8	YFP1	B0015	mRNA	J23100-[BCD8]-YFP1
J23100	BNonTS	YFP1	B0015	Switch	J23100-[BNonTS]-YFP1
J23100	CFP1-TS1	YFP1	B0015	Switch	J23100-[CFP1-TS1]-YFP1
J23100	CFP1-TS2	YFP1	B0015	Switch	J23100-[CFP1-TS2]-YFP1
J23100	GFP1-TS1	YFP1	B0015	Switch	J23100-[GFP1-TS1]-YFP1
J23100	GFP1-TS2	YFP1	B0015	Switch	J23100-[GFP1-TS2]-YFP1
J23100	GFP1-TS3	YFP1	B0015	Switch	J23100-[GFP1-TS3]-YFP1
J23100	RFP1-TS1	YFP1	B0015	Switch	J23100-[RFP1-TS1]-YFP1
J23100	RFP1-TS2	YFP1	B0015	Switch	J23100-[RFP1-TS2]-YFP1
J23100	YFP1-TS1	YFP1	B0015	Switch	J23100-[YFP1-TS1]-YFP1
J23100	YFP1-TS2	YFP1	B0015	Switch	J23100-[YFP1-TS2]-YFP1

Level 1 (transcriptional units) constructs assembled and characterized in the plate reader experiments. It is a subset of the 93 Level 1 constructs built during this research, with the rest omitted from this study.

Table 14. Level 2 Constructs

Toehold Construct	**Spacer**	**Target mRNA**	**Spacer**	**Sequencing**
J23100-[CFP1-TS1]-RFP1	36INS2	J23106-B0034-CFP1	36INS7	Confirmed
J23100-[CFP1-TS1]-RFP1	36INS2	J23106-B0034-YFP1	36INS7	Incorrect
J23100-[CFP1-TS1]-RFP1	36INS2	J23106-B0034-GFP1	36INS7	Incorrect
J23100-[YFP1-TS1]-RFP1	36INS2	J23106-B0034-CFP1	36INS7	Confirmed
J23100-[YFP1-TS1]-RFP1	36INS2	J23106-B0034-YFP1	36INS7	Confirmed
J23100-[YFP1-TS1]-RFP1	36INS2	J23106-B0034-GFP1	36INS7	Incorrect
J23100-[GFP1-TS1]-RFP1	36INS2	J23106-B0034-CFP1	36INS7	Confirmed
J23100-[GFP1-TS1]-RFP1	36INS2	J23106-B0034-YFP1	36INS7	Incorrect
J23100-[GFP1-TS1]-RFP1	36INS2	J23106-B0034-GFP1	36INS7	Incorrect
J23100-[GFP1-TS2]-RFP1	36INS2	J23106-B0034-CFP1	36INS7	Confirmed
J23100-[GFP1-TS2]-RFP1	36INS2	J23106-B0034-YFP1	36INS7	Confirmed
J23100-[GFP1-TS2]-RFP1	36INS2	J23106-B0034-GFP1	36INS7	Confirmed
J23100-[RFP1-TS1]-GFP1	36INS2	J23106-B0034-RFP1	36INS7	Confirmed
J23100-B0034-GFP1	36INS2	J23106-B0034-RFP1	36INS7	Incorrect
J23100-B0034-RFP1	36INS2	J23106-B0034-CFP1	36INS7	Incorrect
J23100-B0034-RFP1	36INS2	J23106-B0034-YFP1	36INS7	Incorrect
J23100-B0034-RFP1	36INS2	J23106-B0034-GFP1	36INS7	Incorrect

Level 2 assemblies (multi-transcriptional units) into pSB3C03. These assemblies used toehold constructs (or controls), spacers, and target mRNA constructs. Of 17 different Level 2 assemblies, only 8 were sequence confirmed.

Table 15. Conversion for Comparable Units

	MEFL / a.u.	**Silica Particles**	**Conversion Factor**
Experiment 1	5.49E+10	8.63E+07	636
Experiment 2	5.60E+10	9.96E+07	562
	MERH / a.u.	**Silica Particles**	**Conversion Factor**
Experiment 1	2.77E+10	8.63E+07	636
Experiment 2	2.49E+10	9.96E+07	562

Data from standard curves for the conversion of arbitrary units (a.u) to MEFL, molecules of equivalent fluorescein, or MERH, molecules of equivalent rhodamine. Silica particle counts reflect the mean of med-high levels from serial dilution. Data calcuated with a modified 2018 Interlab excel sheet (iGEM 2018 InterLab, 2018)

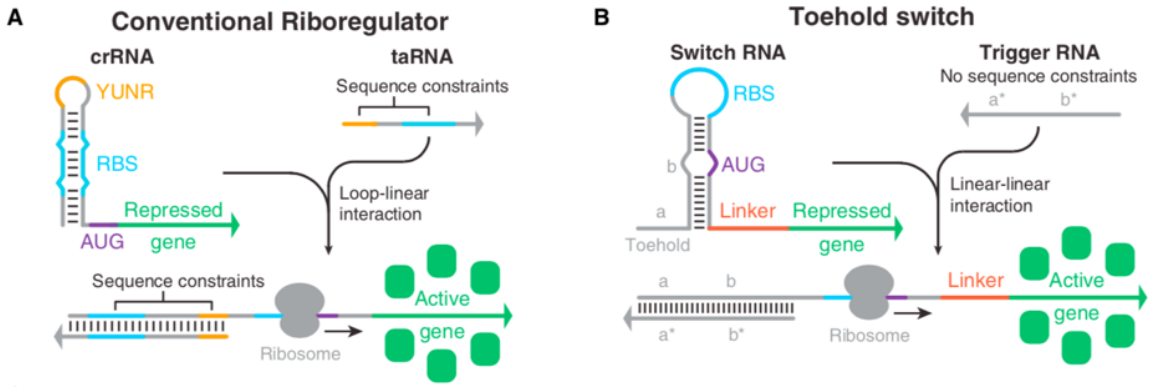

Figure 5. Conventional riboregulator and toehold switch comparison.

(A) Design of a conventional riboregulator (Isaacs et al., 2004), demonstrating crRNA stem-loop structure which sequesters ribosome binding site (RBS). An added taRNA will complementarily bind to the crRNA to allow for the ribosome to bind, and translation to be initiated. crRNA and taRNA sequence constraints are shown in color, while variable sequences are in gray.
(B) Design of a toehold switch, demonstrating switch RNA stem-loop. An added trigger RNA will complementarily bind to the switch to allow for the ribosome to bind, and translation initiation. Compared to the conventional riboregulator, the switch and trigger interaction can support greater variable sequences (in gray). (Green et al., 2014)

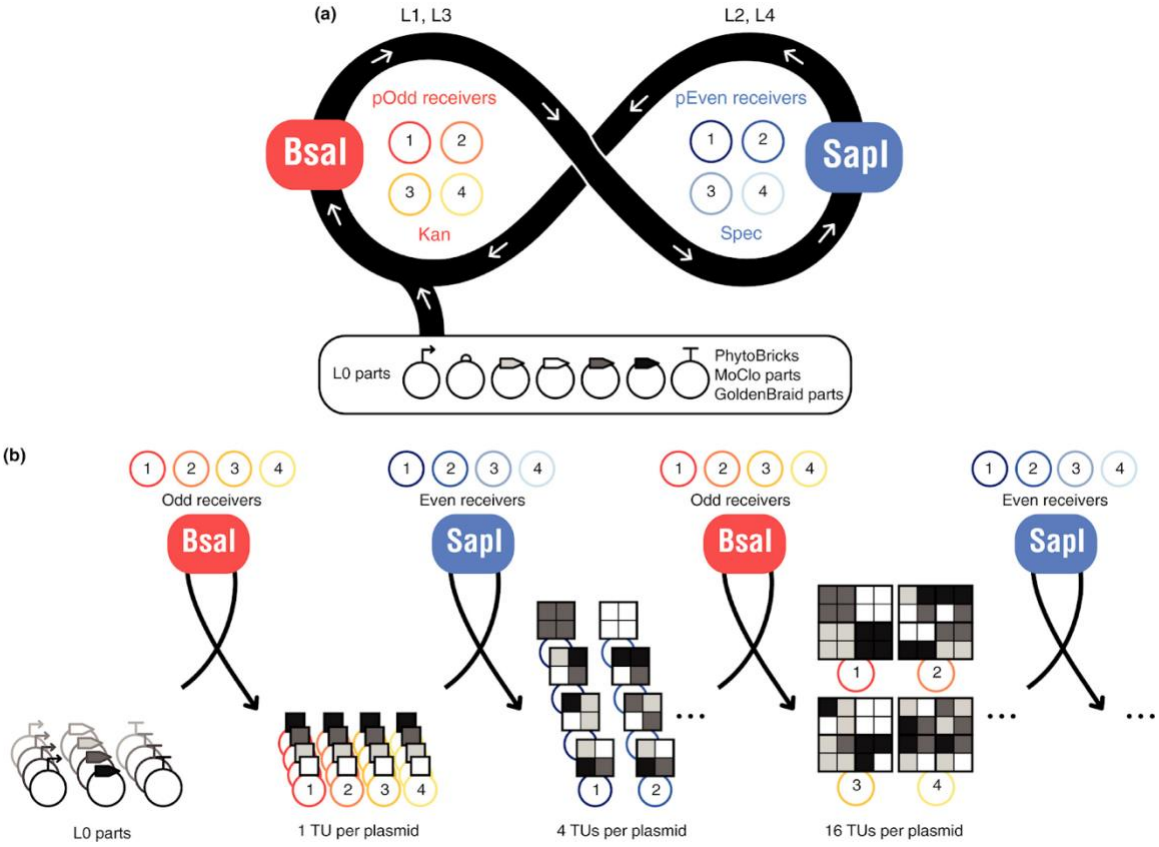

Figure 6. Loop assembly overview

The recursive approach to Type IIS assembly, alternating between two restriction enzymes, Bsa1 and Sap1, to build large genetic circuits. (Pollack et al., 2018)

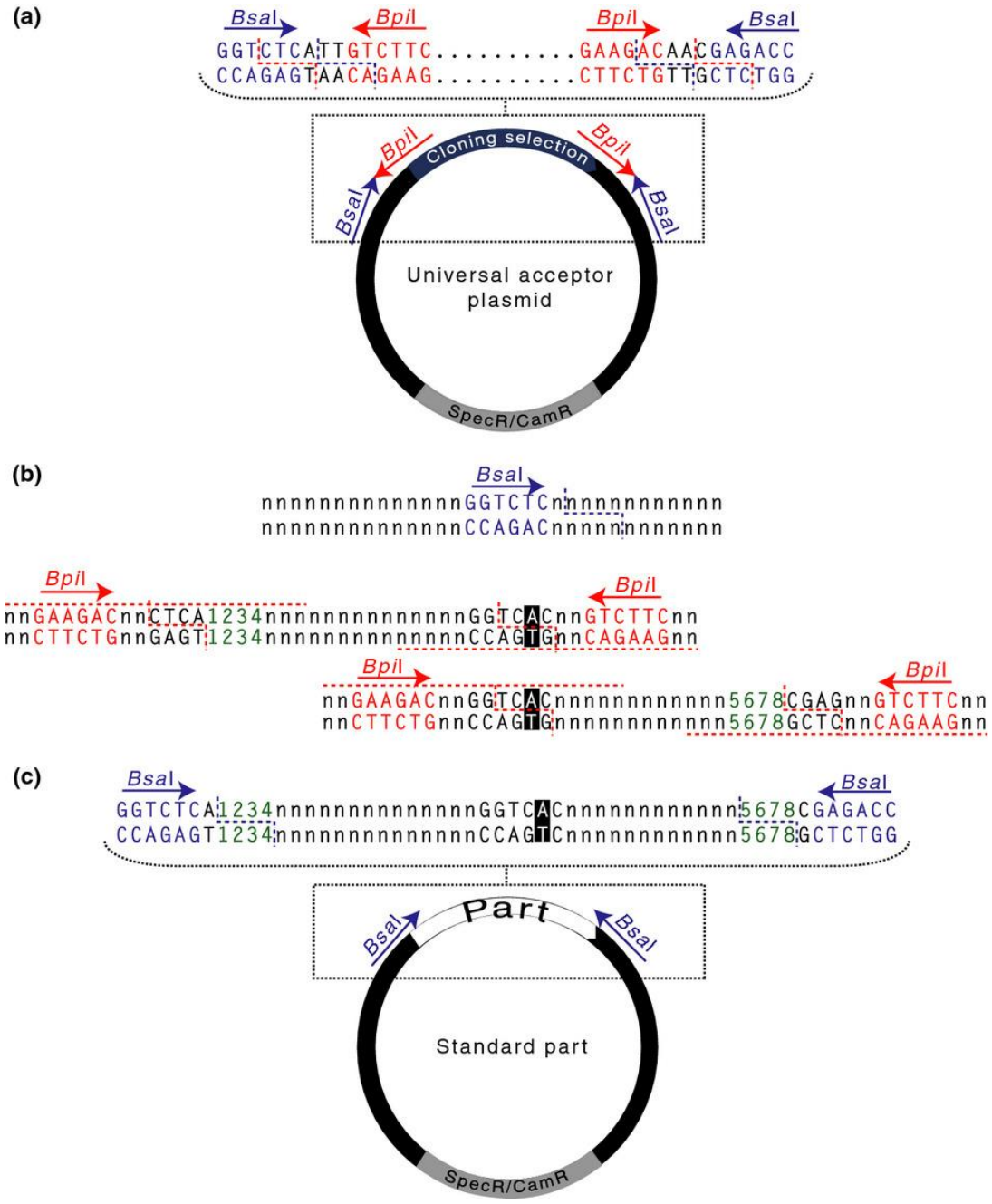

Figure 7. PhytoBrick Universal Acceptor Plasmid

The design of this plasmid allows for the cloning of Type IIS parts with any desired 4 base pair fusion sites. Parts are selected for against the cloning selection marker on the plasmid (Patron et al., 2015).

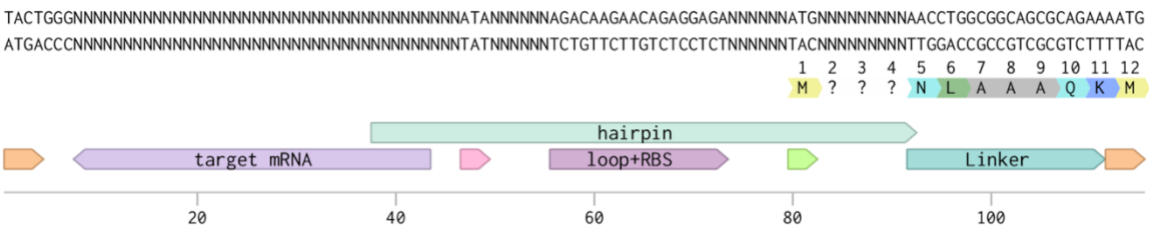

Figure 8. Toehold Switch Template Structure

The following figure denotes the template structure and sequence of the toehold switch based on Green et al. In orange, the 5' and 3' Type IIS Fusion Site. In yellow, the start codon. The hairpin structure consists of 9 base pairs of binding, an unbound start codon, 6 base pairs of binding, followed by the loop structure containing the RBS. Image produced in Benchling (http://benchling.com).

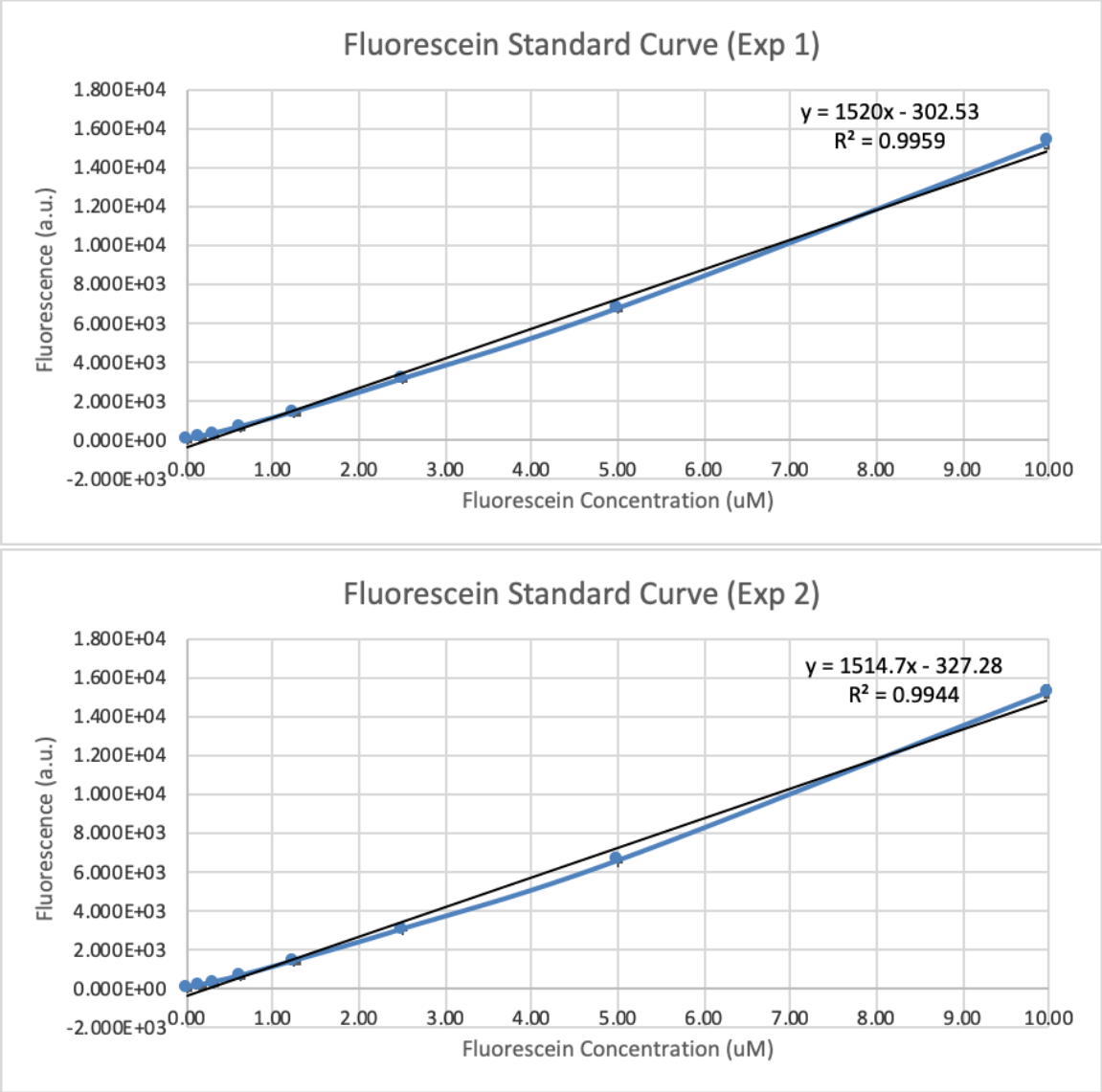

Figure 9. Fluorescein Standard Curves

Fluorescein data from plate reader calibration prior to experiments 1 and 2. Data reflects filter setting 1 from Table 5. Linear regression is expected and demonstrates proper serial dilution and desired range of values. Data calculated and graphed with a modified 2018 InterLab excel sheet (iGEM 2018 InterLab, 2018).

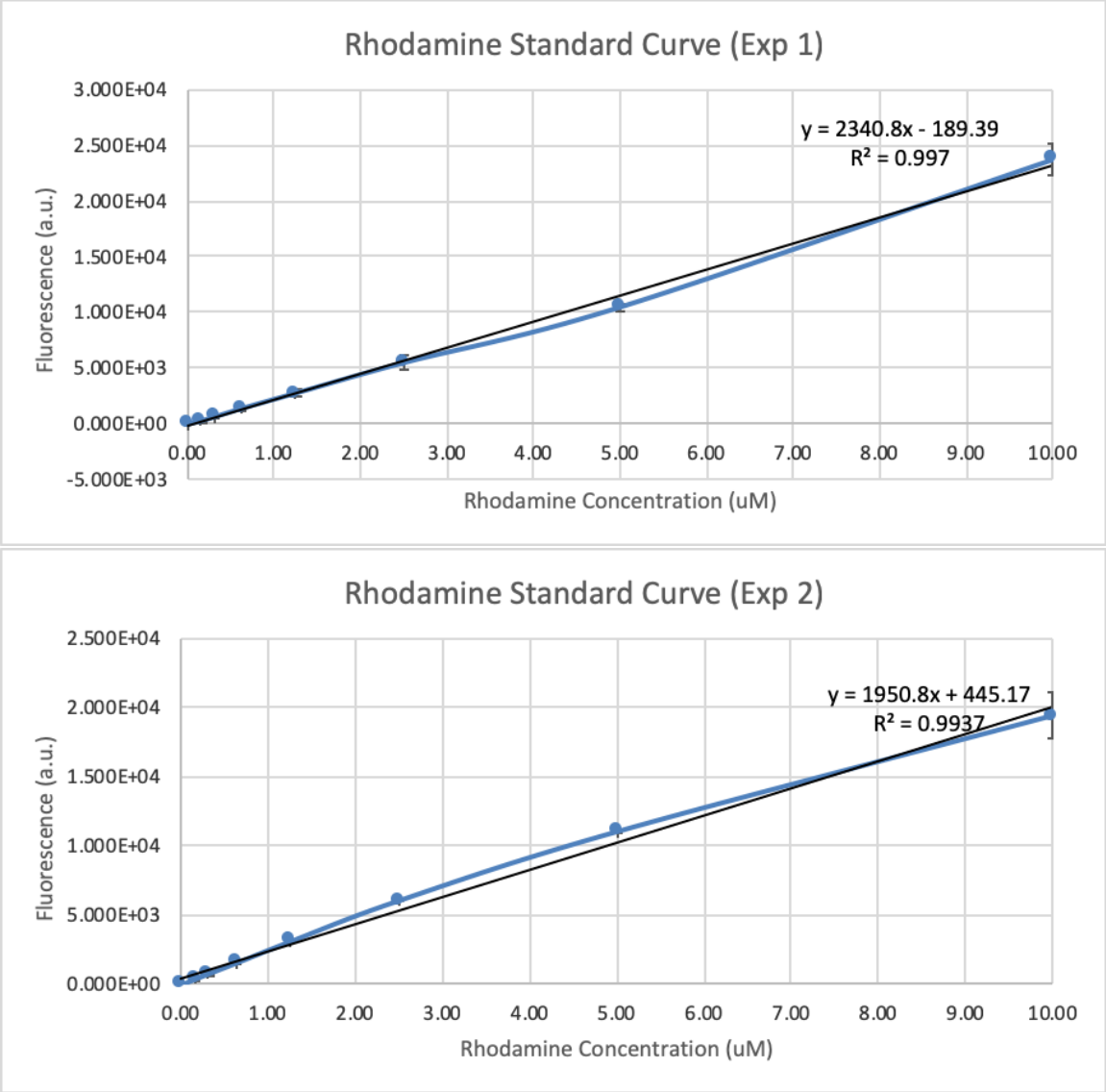

Figure 10. Rhodamine B Standard Curves

Rhodamine B data from plate reader calibration prior to experiments 1 and 2. Data reflects filter setting 3 from Table 5. Linear regression is expected and demonstrates proper serial dilution and desired range of values. Data calculated and graphed with a modified 2018 InterLab excel sheet (iGEM 2018 InterLab, 2018).

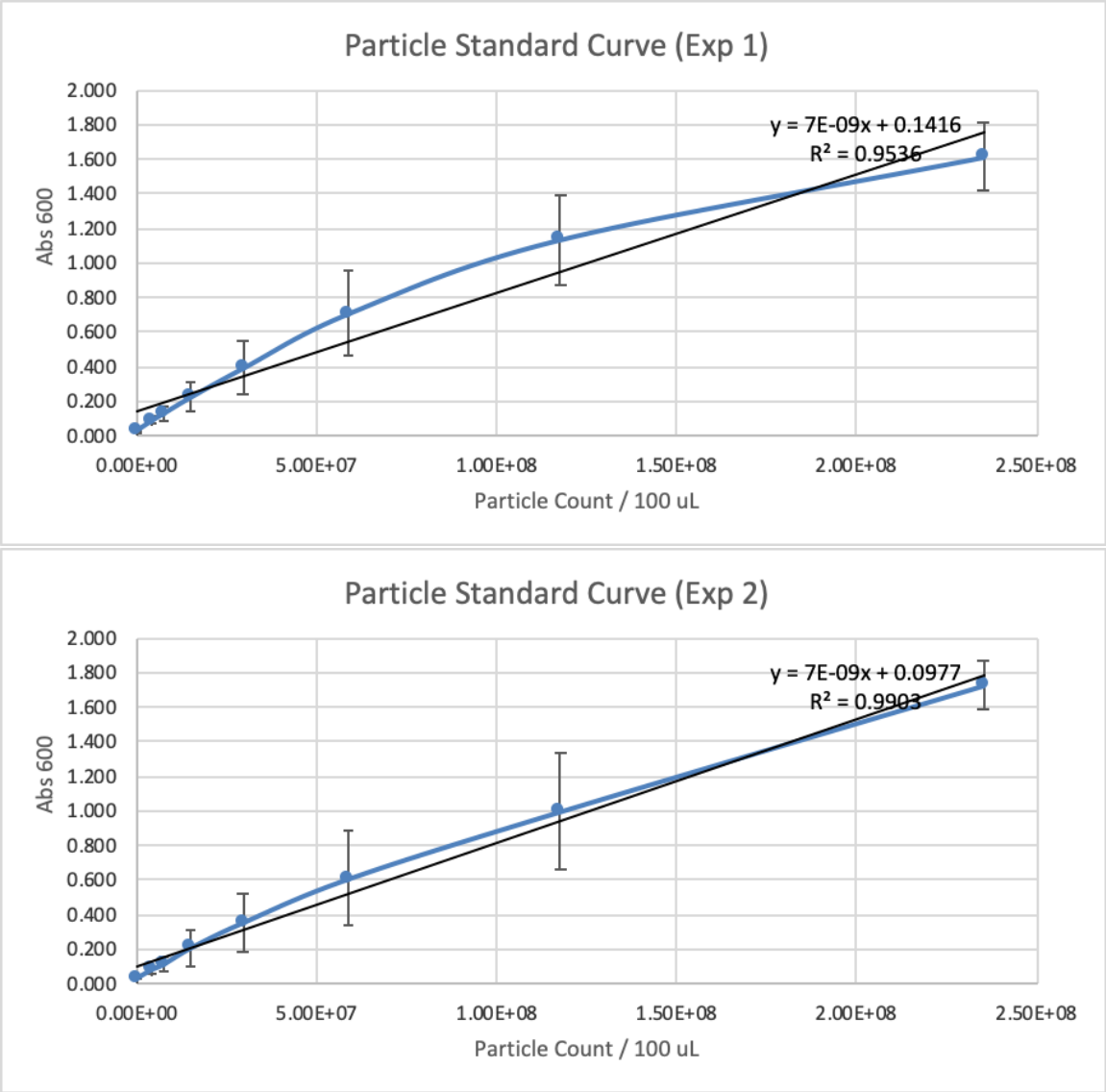

Figure 11. Silica Microspheres Standard Curves

Silica microspheres data from plate reader calibration prior to experiments 1 and 2. Data reflects absorbance at 600nm. Linear regression is expected and demonstrates proper serial dilution and desired range of values. Data calculated and graphed with a modified 2018 InterLab excel sheet (iGEM 2018 InterLab, 2018).

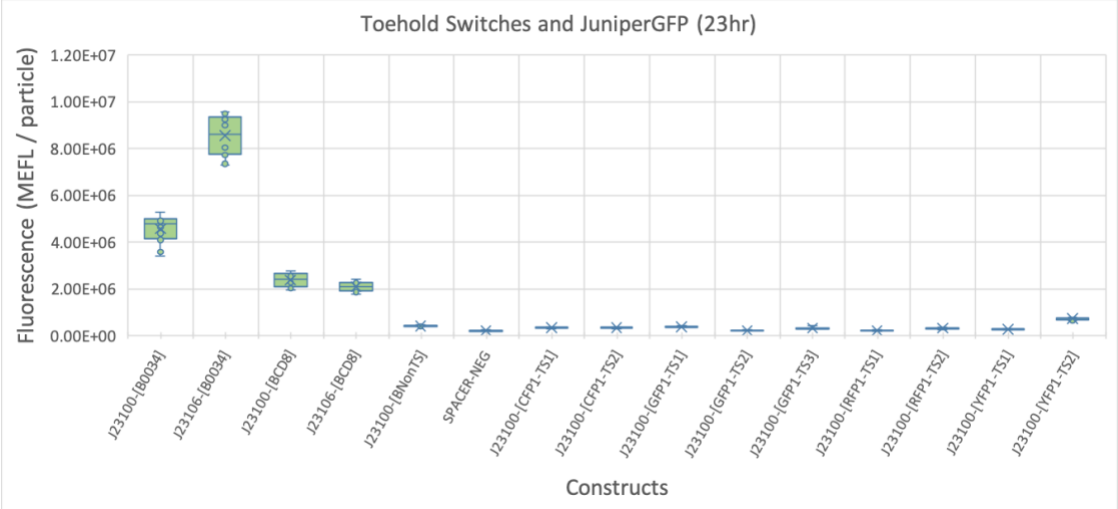

Figure 12. Toehold Switches paired with JuniperGFP at 23 hr.

Fluorescence (a.u) and absorption collected using filter setting 1 on Table 5 and converted to MEFL per particle. Per construct, all replicates from both plate reader experiments are represented ±SD. n=18 per datapoint

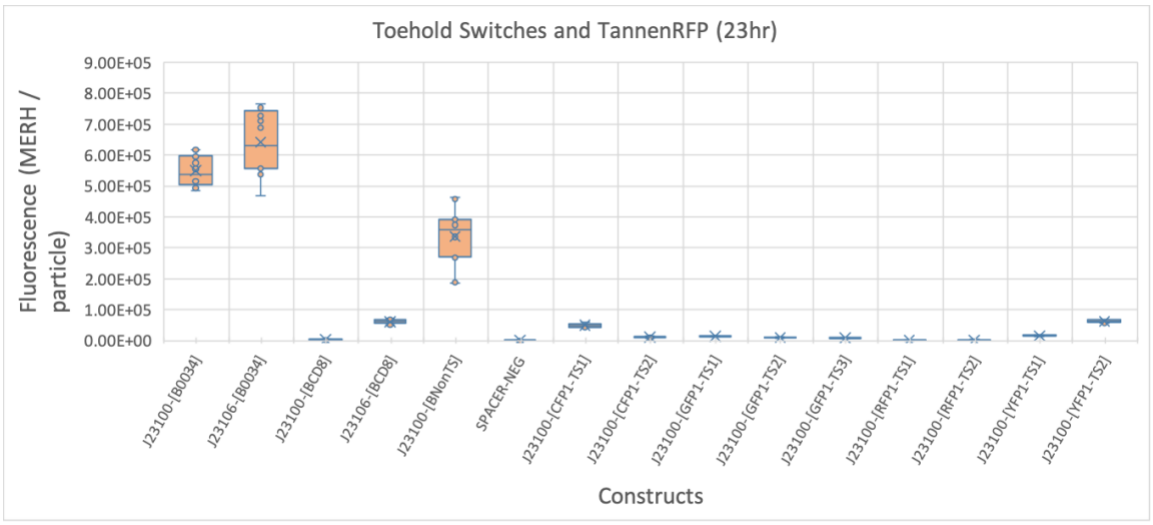

Figure 13. Toehold Switches paired with TannenRFP at 23 hr.

Fluorescence (a.u) and absorption collected using filter setting 3 on Table 5 and converted to MERH per particle. Per construct, all replicates from both plate reader experiments are represented ±SD. n=18 per datapoint

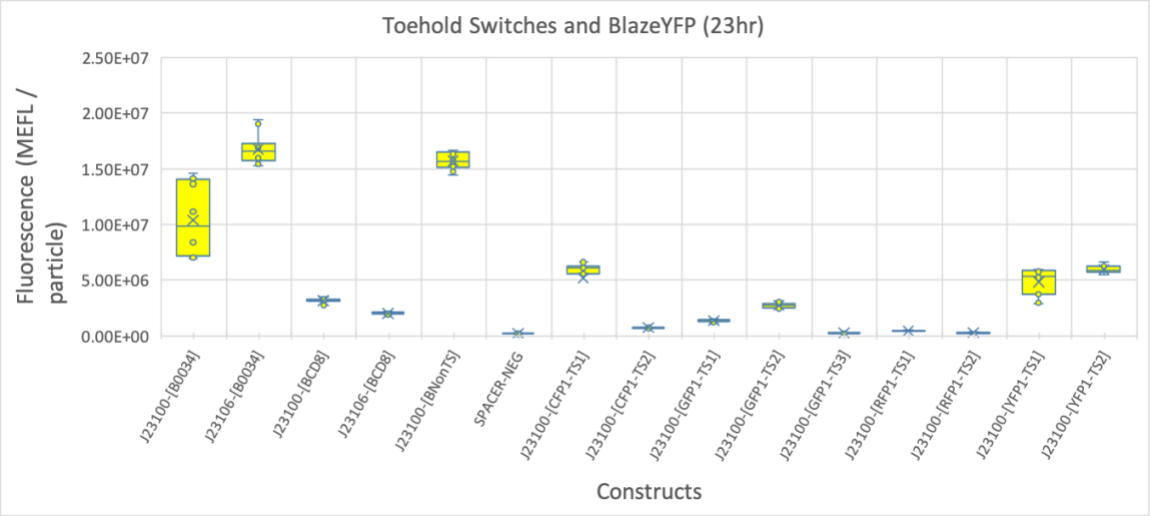

Figure 14. Toehold Switches paired with BlazeYFP at 23 hr.

Fluorescence (a.u) and absorption collected using filter setting 1 on Table 5 and converted to MEFL per particle. Per construct, all replicates from both plate reader experiments are represented ±SD. n=18 per datapoint

References

Beal, J., Haddock-Angelli, T., Gershater, M., Mora, K. D., Lizarazo, M., Hollenhorst, J., & Rettberg, R. (2016) Reproducibility of Fluorescent Expression from Engineered Biological Constructs in E. coli. *PLoS ONE* 11(3): e0150182. https://doi.org/10.1371/journal.pone.0150182

Beal, J., Haddock-Angelli, T., Baldwin, G., Gershater, M., Dwijayanti, A., Mora, K. D., Lizarazo, M., & Rettberg, R. (2018). Quantification of bacterial fluorescence using independent calibrants. *PLoS ONE* 13(6): e0199432. https://doi.org/10.1371/journal.pone.0199432

Brantl, S., & Wagner, E. G. (2002). Antisense RNA-mediated transcriptional attenuation: an in vitro study of plasmid pT181. *Molecular Microbiology*, 35(6), 1469-1482.

Cameron, D. E., Bashor, C. J., & Collins, J. J. (2014). A brief history of synthetic biology. *Nature Reviews Microbiology*, 12(5), 381-390.

Carr, S. B., Beal, J., & Densmore, D. M. (2017). Reducing DNA context dependence in bacterial promoters. *PloS ONE*, 12(4), e0176013. doi:10.1371/journal.pone.0176013

Chakravarti, D., Cho, J. H., Weinberg, B. H., Wong, N. M., & Wong, W. W. (2016). Synthetic biology approaches in cancer immunotherapy, genetic network engineering, and genome editing. *Integrative Biology*, 8(4), 504-517.

Day, R. N., & Davidson, M. W. (2009). The fluorescent protein palette: tools for cellularimaging. *Chemical Society Reviews*, 38(10), 2887.

Ellis, T., Adie, T., & Baldwin, G. S. (2011). DNA assembly for synthetic biology: from parts to pathways and beyond. *Integrative Biology*, 3(2), 109.

Elowitz, M. B., & Leibler, S. (2000). A synthetic oscillatory network of transcriptionalregulators. *Nature*, 403(6767), 335-338.

Engler, C., Kandzia, R., & Marillonnet, S. (2008). A One Pot, One Step, Precision Cloning Method with High Throughput Capability. *PLoS ONE*, 3(11).

Gardner, T. S., Cantor, C. R., & Collins, J. J. (2000). Construction of a genetic toggle switch in Escherichia coli. *Nature*, 403(6767), 339-342.

Green, A., Silver, P., Collins, J., & Yin, P. (2014). Toehold Switches: De-Novo-DesignedRegulators of Gene Expression. *Cell, 159*(4), 925-939.

Green, A. A., Kim, J., Ma, D., Silver, P. A., Collins, J. J., & Yin, P. (2017). Complex cellular logic computation using ribocomputing devices. *Nature*, 548(7665), 117-121.

Hanahan, D. (1983). Studies on transformation of Escherichia coli with plasmids. *Journal of Molecular Biology*, 166(4), 557-580.

Hasty, J., Mcmillen, D., & Collins, J. J. (2002). Engineered gene circuits. *Nature*, 420(6912), 224-230.

Isaacs, F. J., Dwyer, D. J., Ding, C., Pervouchine, D. D., Cantor, C. R., & Collins, J. J. (2004). Engineered riboregulators enable post-transcriptional control of gene expression. *Nature Biotechnology*, 22(7), 841-847.

Iverson, S. V., Haddock, T. L., Beal, J., & Densmore, D.M. (2016). CIDAR MoClo: Improved MoClo Assembly Standard and New E. coli Part Library Enable Rapid Combinatorial Design for Synthetic and Traditional Biology. *ACS Synthetic Biology*. Jan 15;5(1):99-103. pmid:26479688 doi: 10.1021/acssynbio.5b00124

Jacob, F., & Monod, J. (1961). On the Regulation of Gene Activity. *Cold Spring HarborSymposia on Quantitative Biology*, 26(0), 193-211.

Kelly, J. R., Rubin, A. J., Davis, J. H., Ajo-Franklin, C.M., Cumbers, J., Czar, M.J., Mora, K. D., Glieberman, A. L, Monie, D. D., & Endy, D. (2009). Measuring the activity of BioBrick promoters using an in vivo reference standard. *Journal of Biological Engineering*, 3(4). pmid:19298678

Knight, T. (2003). Idempotent Vector Design for Standard Assembly of Biobricks.

Mizuno, T., Chou, M. Y., & Inouye, M. (1984). A Unique Mechanism Regulating Gene Expression: Translational Inhibition by a Complementary RNA Transcript (micRNA). *Proceedings of the National Academy of Sciences*, 81(13), 4240-4240.

Nielsen, J., Larsson, C., Maris, A. V., & Pronk, J. (2013). Metabolic engineering of yeast for production of fuels and chemicals. *Current Opinion in Biotechnology*, 24(3), 398-404.

Pardee, K., Green, A., Ferrante, T., Cameron, D., Daleykeyser, A., Yin, P., & Collins, J. (2014). Paper-Based Synthetic Gene Networks. *Cell*, 159(4), 940-954.

Patron, N. J., Orzaez, D., Marillonnet, S., Warzecha, H., Matthewman, C., Youles, M., Raitskin, O., Leveau, A., Farré, G., Rogers, C., Smith, A., Hibberd, J., Webb, A. A., Locke, J., Schornack, S., Ajioka, J., Baulcombe, D. C., Zipfel, C., Kamoun, S., Jones, J. D., Kuhn, H., Robatzek, S., Van Esse, H. P., Sanders, D., Oldroyd, G., Martin, C., Field, R., O'Connor, S., Fox, S., Wulff, B., Miller, B., Breakspear, A., Radhakrishnan, G., Delaux, P., Loqué, D., Granell, A., Tissier, A., Shih, P., Brutnell, T. P., Quick, W. P., Rischer, H., Fraser, P. D., Aharoni, A., Raines, C., South, P. F., Ané, J., Hamberger, B. R., Langdale, J., Stougaard, J., Bouwmeester, H., Udvardi, M., Murray, J. A., Ntoukakis, V., Schäfer, P., Denby, K., Edwards, K. J., Osbourn, A. and Haseloff, J. (2015), Standards for plant synthetic biology: a common syntax for exchange of DNA parts. *New Phytologist*, 208: 13-19. doi:10.1111/nph.13532

Peters, G., Maertens, J., Lammertyn, J., & De Mey, M. (2018) Exploring of the feature space of *de novo* developed post-transcriptional riboregulators. *PLOS Computational Biology* 14(8): e1006170. https://doi.org/10.1371/journal.pcbi.1006170

Pollak, B., Cerda, A., Delmans, M., Álamos, S., Moyano, T., West, A., Gutiérrez, R. A., Patron, N. J., Federici, F., and Haseloff, J. (2019), Loop assembly: a simple and open system for recursive fabrication of DNA circuits. *New Phytologist*, 222: 628-640. doi:10.1111/nph.15625

Purnick, P. E., & Weiss, R. (2009). The second wave of synthetic biology: from modules to systems. *Nature Reviews Molecular Cell Biology*, 10(6), 410-422.

Shetty, R. P., Endy, D., & Knight, T. F. (2008) Engineering BioBrick vectors from BioBrick parts. *Journal of Biological Engineering.* 2(1):1–12.

Siuti, P., Yazbek, J., & Lu, T. K. (2013). Synthetic circuits integrating logic and memory in living cells. *Nature Biotechnology*, 31(5), 448-452.

Stanton, B. C., Nielsen, A. A., Tamsir, A., Clancy, K., Peterson, T., & Voigt, C. A. (2013). Genomic mining of prokaryotic repressors for orthogonal logic gates. *Nature Chemical Biology*, 10(2), 99-105.

To, A. C., Chu, D. H., Wang, A. R., Li, F. C., Chiu, A. W., Gao, D. Y., Choi, C. H. J., Kong, S. K., Chan, T. F., Chan, K. M., & Yip, K. Y. (2018). A comprehensive web tool for toehold switch design. *Bioinformatics, 34*(16), 2862-2864. doi:10.1093/bioinformatics/bty216

Weber, E., Engler, C., Gruetzner, R., Werner, S., & Marillonnet, S. (2011). A Modular Cloning System for Standardized Assembly of Multigene Constructs. *PLoS ONE*, 6(2).

Protocols and Webpages

Annealing and primer extension with Taq polymerase. (2006). Retrieved from https://openwetware.org/wiki/Knight:Annealing_and_primer_extension_with_Taq_polymerase

iGEM 2018 InterLab Study Protocol. (2018). [PDF file]. Retrieved from http://2018.igem.org/wiki/images/0/09/2018_InterLab_Plate_Reader_Protocol.pdf

Type IIS. (2019). Retrieved from http://parts.igem.org/Help:Standards/Assembly/Type_IIS

Transformation. (2017). Retrieved from http://parts.igem.org/Help:Protocols/Transformation

BBa_B0015. (2003, July 17). Retrieved from http://parts.igem.org/Part:BBa_B0015

BBa_J97000. (2014, February 4). Retrieved from http://parts.igem.org/Part:BBa_J97000

BBa_J97001. (2014, February 18). Retrieved from http://parts.igem.org/Part:BBa_J97001

BBa_J97002. (2014, February 18). Retrieved from http://parts.igem.org/Part:BBa_J97002

BBa_J97003. (2014, February 18). Retrieved from http://parts.igem.org/Part:BBa_J97003

BBa_J04450. (2005, June 9). Retrieved from http://parts.igem.org/Part:BBa_J04450

pSB1C3. (2008, September 8). Retrieved from http://parts.igem.org/Part:pSB1C3

pSB1K3. (2008, September 8). Retrieved from parts.igem.org/Part:pSB1K3

pSB3C5. (2007, April 11). http://parts.igem.org/Part:pSB3C5